# “The fundamental problems and high $p_T$ physics in the energy range $\sqrt{s_{NN}}$ < 10 GeV”

*Shimanskiy S.S. (JINR)*

# Nonperturbative QCD problems and the lightest quarks

| | |
|---|---|
| Quark-partons | m=0 |
| Current quarks | m ~ MeV |
| Constituent quarks | m ~ 100 MeV |
| Confinement | Laws ? |
| Hadronization | q -> meson ~ 100% |

Volume 8, number 3 PHYSICS LETTERS 1 February 1964

Multiquark states have been discussed since the 1st page of the quark model

# A SCHEMATIC MODEL OF BARYONS AND MESONS *

M. GELL-MANN
*California Institute of Technology, Pasadena, California*

Received 4 January 1964

If we assume that the strong interactions of baryons and mesons are correctly described in terms of the broken "eightfold way" [1-3], we are tempted to look for some fundamental explanation of the situation. A highly promised approach is the purely dynamical "bootstrap" model for all the strongly interacting particles within which one may try to derive isotopic spin and strangeness conservation and broken eightfold symmetry from self-consistency alone [4]. Of course, with only strong interactions, the orientation of the asymmetry in the unitary space cannot be specified; one hopes that in some way the selection of specific components of the F-spin by electromagnetism and the weak interactions determines the choice of isotopic spin and hypercharge directions.

Even if we consider the scattering amplitudes of strongly interacting particles on the mass shell only and treat the matrix elements of the weak, electromagnetic, and gravitational interactions by means

ber $n_t - n_{\bar{t}}$ would be zero for all known baryons and mesons. The most interesting example of such a model is one in which the triplet has spin $\frac{1}{2}$ and $z = -1$, so that the four particles $d^-$, $s^-$, $u^0$ and $b^0$ exhibit a parallel with the leptons.

A simpler and more elegant scheme can be constructed if we allow non-integral values for the charges. We can dispense entirely with the basic baryon b if we assign to the triplet t the following properties: spin $\frac{1}{2}$, $z = -\frac{1}{3}$, and baryon number $\frac{1}{3}$. We then refer to the members $u^{\frac{2}{3}}$, $d^{-\frac{1}{3}}$, and $s^{-\frac{1}{3}}$ of the triplet as "quarks" [6] $q$ and the members of the anti-triplet as anti-quarks $\bar{q}$. Baryons can now be constructed from quarks by using the combinations $(q\,q\,q)$, $(q\,q\,q\,q\,\bar{q})$, etc., while mesons are made out of $(q\,\bar{q})$, $(q\,q\,\bar{q}\,\bar{q})$, etc. It is assuming that the lowest baryon configuration $(q\,q\,q)$ gives just the representations **1**, **8**, and **10** that have been observed, while the lowest meson configuration $(q\,\bar{q})$ similarly gives just **1** and **8**.

that it would never have been detected. A search for stable quarks of charge $-\frac{1}{3}$ or $+\frac{2}{3}$ and/or stable di-quarks of charge $-\frac{2}{3}$ or $+\frac{1}{3}$ or $+\frac{4}{3}$ at the highest energy accelerators would help to reassure us of the non-existence of real quarks.

# Status of the pentaquark problem

- 1st relatively certain theoretical suggestion
  of mass ~1530 MeV and width < 15 MeV :
  Diakonov, Petrov, Polyakov, Z.Phys., A**359** (1997) 305.
- Experiment : about ten papers with positive evidences;
  about ten papers with negative results
  (some of them with higher statistics ).
- Common opinion and PDG position
  (since edition of 2008) :
  Pentaquark is dead !
  (Note, at the same time, great enthusiasm
  in searches for tetraquarks ! )

Phys.Atom.Nucl. 74 (2011) 418-425

ЯДЕРНАЯ ФИЗИКА, 2011, том 74, № 3, с. 438–446

ЭЛЕМЕНТАРНЫЕ ЧАСТИЦЫ И ПОЛЯ

# QUARK–DIQUARK SYSTEMATICS OF BARYONS: SPECTRAL INTEGRAL EQUATIONS FOR SYSTEMS COMPOSED BY LIGHT QUARKS

© 2011 A. V. Anisovich, V. V. Anisovich*,
M. A. Matveev, V. A. Nikonov, A. V. Sarantsev, T. O. Vulfs
*Petersburg Nuclear Physics Institute, Russian Academy of Sciences, Gatchina*
Received May 7, 2010; in final form, August 30, 2010

PHYSICAL REVIEW D 94, 034039 (2016)

# How Often Do Diquarks Form? A Very Simple Model

Richard F. Lebed*
*Department of Physics, Arizona State University, Tempe, Arizona 85287-1504, USA*
(Dated: June, 2016)

Starting from a textbook result, the nearest-neighbor distribution of particles in an ideal gas, we develop estimates for the probability with which quarks $q$ in a mixed $q$, $\bar{q}$ gas are more strongly attracted to the nearest $q$, potentially forming a diquark, than to the nearest $\bar{q}$. Generic probabilities lie in the range of tens of percent, with values in the several percent range even under extreme assumptions favoring $q\bar{q}$ over $qq$ attraction.

We have seen that the large relative size of the short-distance attraction between quarks in the color-antitriplet channel compared to the attraction between a quark and an antiquark in the color-singlet channel leads inexorably to a given quark being initially attracted to a quark rather than an antiquark a sizeable fraction of the time. We interpret this initial attraction as the seed event in the formation of a compact diquark $qq$ rather than a color-singlet $q\bar{q}$ pair.

# Hadrons from diquarks?

Still an open question!

**Role of diquarks in building hadrons?**

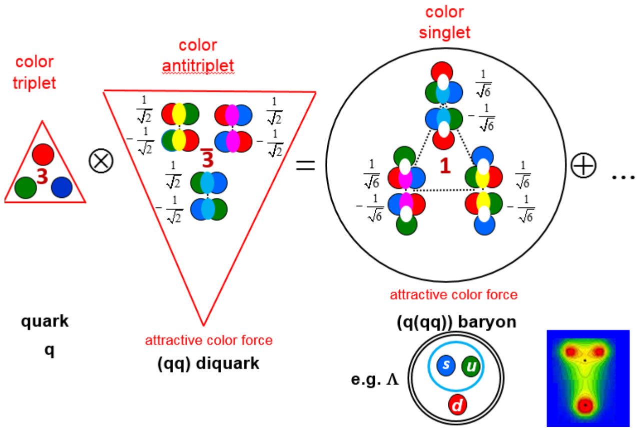


vs.

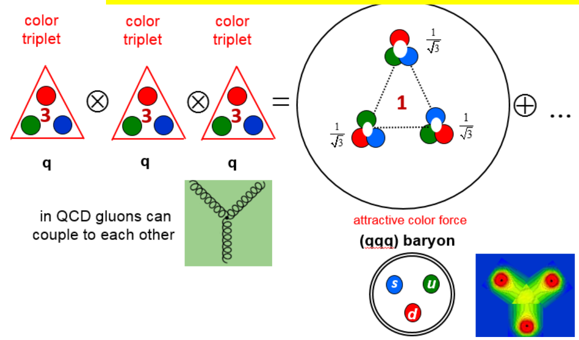


**Light and heavy baryon spectroscopy is sensitive to this question**

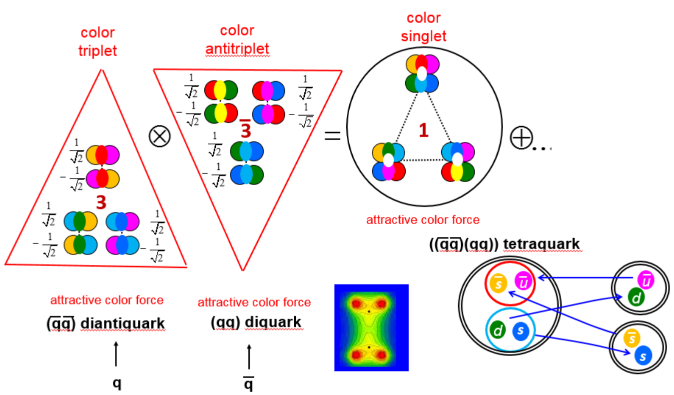


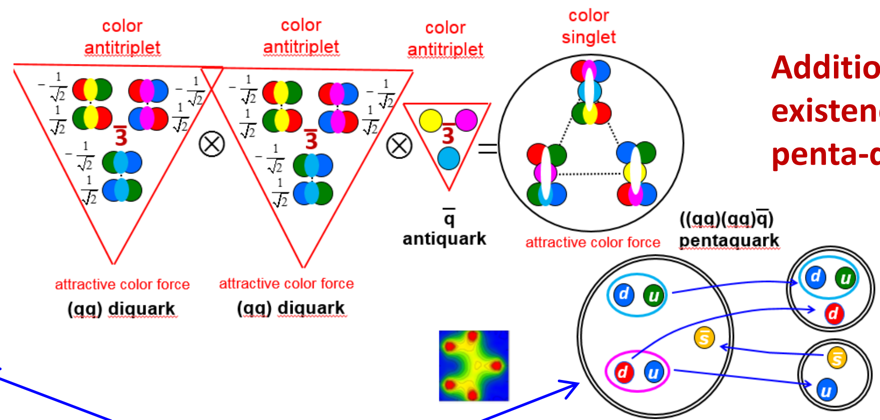


**Additional motivation for existence of tetra- and penta-quarks.**

Exotic Hadrons, Dubna, Sep.18,2018 Tomasz Skwarnicki

**Does effective mechanism to suppress rapid fall-apart exist?**

# DIQUARK DYNAMICS

# Why high $p_T$ is needed?

# The Counting Rules

**We deal with dominance of constituent quarks**

## Two articles in 1973 were published:

*Matveev V.A., Muradyan R.M., Tavkhelidze A.N.* ***Lett. Nuovo Cimento 7,719 (1973);***

*Brodsky S., Farrar G.* ***Phys. Rev. Lett. 31,1153 (1973)***

Predictions that for momentum $p_{beam} \geq 5$ GeV/c in any binary large-angle scattering ($\theta_{cm} > 40°$) reactions at large momentum transfers $Q = \sqrt{-t}$ :

$$A + B \to C + D$$

$$\left.\frac{d\sigma}{dt}\right|_{A+B\to C+D} \sim s^{-(n_A+n_B+n_C+n_D-2)} f\left(\frac{t}{s}\right)$$

where $n_A$, $n_B$, $n_C$ and $n_D$ the amounts of elementary constituents in A,B,C and D.

$s=(p_A+p_B)^2$ and $t=(p_A-p_C)^2$,

$$\left.\frac{d\sigma}{dt}\right|_{pp\to pp} \sim s^{-10} \quad \text{and} \quad \left.\frac{d\sigma}{dt}\right|_{\pi p\to \pi p} \sim s^{-8}$$

# Comparison of 20 exclusive reactions at large $t$

TABLE V. The scaling between E755 and E838 has been measured for eight meson-baryon and 2 baryon-baryon interactions at $\theta_{c.m.} = 90°$. The nominal beam momentum was 5.9 GeV/$c$ and 9.9 GeV/$c$ for E838 and E755, respectively. There is also an overall systematic error of $\Delta n_{syst} = \pm 0.3$ from systematic errors of ±13% for E838 and ±9% for E755.

| | | Cross section | | $n$-2 |
|---|---|---|---|---|
| No. | Interaction | E838 | E755 | ($\frac{d\sigma}{dt} \sim 1/s^{n-2}$) |
| 1 | $\pi^+ p \to p\pi^+$ | $132 \pm 10$ | $4.6 \pm 0.3$ | $6.7 \pm 0.2$ |
| 2 | $\pi^- p \to p\pi^-$ | $73 \pm 5$ | $1.7 \pm 0.2$ | $7.5 \pm 0.3$ |
| 3 | $K^+ p \to pK^+$ | $219 \pm 30$ | $3.4 \pm 1.4$ | $8.3^{+0.6}_{-1.0}$ |
| 4 | $K^- p \to pK^-$ | $18 \pm 6$ | $0.9 \pm 0.9$ | $\geq 3.9$ |
| 5 | $\pi^+ p \to p\rho^+$ | $214 \pm 30$ | $3.4 \pm 0.7$ | $8.3 \pm 0.5$ |
| 6 | $\pi^- p \to p\rho^-$ | $99 \pm 13$ | $1.3 \pm 0.6$ | $8.7 \pm 1.0$ |
| 13 | $\pi^+ p \to \pi^+ \Delta^+$ | $45 \pm 10$ | $2.0 \pm 0.6$ | $6.2 \pm 0.8$ |
| 15 | $\pi^- p \to \pi^+ \Delta^-$ | $24 \pm 5$ | $\leq 0.12$ | $\geq 10.1$ |
| 17 | $pp \to pp$ | $3300 \pm 40$ | $48 \pm 5$ | $9.1 \pm 0.2$ |
| 18 | $\bar{p}p \to p\bar{p}$ | $75 \pm 8$ | $\leq 2.1$ | $\geq 7.5$ |

TABLE I. Measured reactions presented in this paper. The reactions are written as (beam + target) → (spectrometer particle + side particle). Reactions 1, 2, 3, 17, and 18 were measured with either final-state particle in the spectrometer.

| | |
|---|---|
| **Meson-baryon reactions** | |
| 1 | $\pi^+ p \to p\pi^+$ |
| 2 | $\pi^- p \to p\pi^-$ |
| 3 | $K^+ p \to pK^+$ |
| 4 | $K^- p \to pK^-$ |
| 5 | $\pi^+ p \to p\rho^+$ |
| 6 | $\pi^- p \to p\rho^-$ |
| 7 | $K^+ p \to pK^{*+}$ |
| 8 | $K^- p \to pK^{*-}$ |
| 9 | $K^- p \to \pi^- \Sigma^+$ |
| 10 | $K^- p \to \pi^+ \Sigma^-$ |
| 11 | $K^- p \to \Lambda\pi^0$ |
| 12 | $\pi^- p \to \Lambda K^0$ |
| 13 | $\pi^+ p \to \pi^+ \Delta^+$ |
| 14 | $\pi^- p \to \pi^- \Delta^+$ |
| 15 | $\pi^- p \to \pi^+ \Delta^-$ |
| 16 | $K^+ p \to K^+ \Delta^+$ |
| **Baryon-baryon reactions** | |
| 17 | $pp \to pp$ |
| 18 | $\bar{p}p \to p\bar{p}$ |
| 19 | $\bar{p}p \to \pi^+\pi^-$ |
| 20 | $\bar{p}p \to K^+K^-$ |

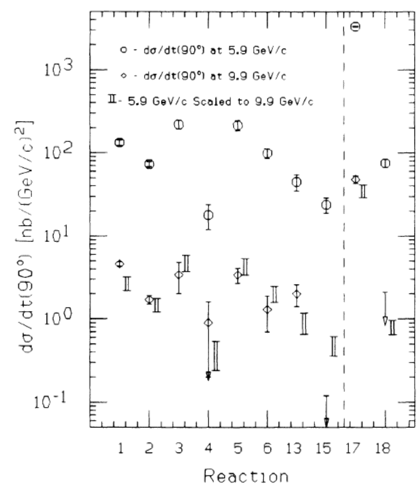


FIG. 26. The scaling between E755 and E838 has been calculated for eight meson-baryon and 2 baryon-baryon interactions at $\theta_{c.m.} = 90°$. The beam momentum for E838 was 5.9 GeV/$c$, corresponding to $s = 11.9$ GeV$^2$ for meson-baryon reactions and $s = 12.9$ GeV$^2$ for baryon-baryon reactions. For the 9.9 GeV/$c$ momentum of E755, the corresponding values of $s$ are 19.6 and 20.5 GeV$^2$.

PHYSICAL REVIEW D VOLUME 10, NUMBER 9 1 NOVEMBER 1974

# Unified description of inclusive and exclusive reactions at all momentum transfers*

R. Blankenbecler and S. J. Brodsky

$$E\frac{d\sigma}{d^3p}(A+B\to C+X)\to(p_T^2)^{-N}f\left(\frac{\mathfrak{M}^2}{s},\frac{t}{s}\right)$$

and[5,6]

$$\frac{d\sigma}{dt}(A+B\to C+D)\to(p_T^2)^{-N}f\left(\frac{t}{s}\right)$$

The entire kinematic range of high-energy inclusive reactions is illustrated on the Peyrou plot of Fig. 1. As usual we define

$$s=(p_A+p_B)^2,\quad t=(p_A-p_C)^2,$$

$$u=(p_B-p_C)^2,\quad \mathfrak{M}^2=(p_A+p_B-p_C)^2,$$

and

$$\epsilon=\mathfrak{M}^2/s\cong(1-p_{\text{c.m.}}/p_{\max}),$$

$$x_T=p_T/p_{\max},\quad x_L=p_L/p_{\max}\simeq(t-u)/s.$$

TABLE I. The expected dominant subprocesses for selected hadronic inclusive reactions at large transverse momentum. The second column lists the important exclusive processes which contribute to each inclusive cross section at $\epsilon\sim0$. The basic subprocesses expected in the CIM, and the resulting form of the inclusive cross section $Ed\sigma/d^3p\sim(p_\perp^2)^{-N}\epsilon^P$ for $p_\perp^2\sim\infty$, $\epsilon\to0$, and fixed $\theta_{\text{c.m.}}$ are given in the last columns. The subprocesses that have the dominant $p_\perp$ dependence at fixed $\epsilon$ are underlined. For some particular final-state quantum numbers, the above powers of $\epsilon$ should be increased.

| Inclusive process | Exclusive-limit channel | Subprocesses | $\frac{d\sigma}{d^3p/E}$ $(\theta\sim90°)$ |
|---|---|---|---|
| $M+B\to M+X$ | $M+B\to M+B^*$ $(n=10)$ | $\underline{M+q\to M+q}$ | $(p_\perp^2)^{-4}\epsilon^3$ |
| | | $\bar q+B\to M+qq$ | $(p_\perp^2)^{-6}\epsilon^1$ |
| | | $M+B\to M+B^*$ | $(p_\perp^2)^{-8}\epsilon^{-1}$ |
| $B+B\to B+X$ | $B+B\to B+B^*$ $(n=12)$ | $\underline{B+q\to B+q}$ | $(p_\perp^2)^{-6}\epsilon^3$ |
| | | $\underline{(qq)+(qq)\to B+q}$ | $(p_\perp^2)^{-6}\epsilon^3$ |
| | | $\underline{B+(qq)\to B+qq}$ | $(p_\perp^2)^{-8}\epsilon^1$ |
| | | $B+B\to B+B^*$ | $(p_\perp^2)^{-10}\epsilon^{-1}$ |
| | $B+B\to B+B^*+M^*$ $(n=14)$ | $\underline{q+q\to B+\bar q}$ | $(p_\perp^2)^{-4}\epsilon^7$ |
| | | $q+(qq)\to B+M^*$ | $(p_\perp^2)^{-6}\epsilon^5$ |
| | | $(qq)+B\to B+M^*+qq$ | $(p_\perp^2)^{-10}\epsilon^1$ |
| | | $B+B\to B+B^*+M^*$ | $(p_\perp^2)^{-12}\epsilon^{-1}$ |
| $B+B\to M+X$ | $B+B\to M+B^*+B^*$ $(n=14)$ | $\underline{q+(qq)\to M+B^*}$ | $(p_\perp^2)^{-6}\epsilon^5$ |
| | | $q+B\to q(\to M+q)+B^*$ | $(p_\perp^2)^{-6}\epsilon^5$ |
| | | $q+B\to M+q+B^*$ | $(p_\perp^2)^{-8}\epsilon^3$ |
| | | $(qq)+B\to M+B^*+qq$ | $(p_\perp^2)^{-10}\epsilon^1$ |
| | | $B+B\to M+B^*+B^*$ | $(p_\perp^2)^{-12}\epsilon^{-1}$ |
| | $B+B\to M+M^*+B^*+B^*$ $(n=16)$ | $\underline{M+q\to M+q}$ | $(p_\perp^2)^{-4}\epsilon^9$ |
| | | $q+q\to\bar q(\to M+\bar q)+B^*$ | $(p_\perp^2)^{-4}\epsilon^9$ |
| | | $q+q\to M+B^*+\bar q$ | $(p_\perp^2)^{-6}\epsilon^7$ |
| | | $M+B\to M+B^*$ | $(p_\perp^2)^{-8}\epsilon^5$ |
| | $B+B\to M+M^*+M^*+B^*+B^*$ $(n=18)$ | $\underline{q+\bar q\to M+M^*}$ | $(p_\perp^2)^{-4}\epsilon^{11}$ |
| | | $\underline{q+M\to q(\to M+q)+M^*}$ | $(p_\perp^2)^{-4}\epsilon^{11}$ |
| $B+B\to\bar B+X$ | $B+B\to\bar B+B^*+B^*+\bar B^*$ $(n=18)$ | $\underline{q+q\to B^*+\bar q(\to\bar B+qq)}$ | $(p_\perp^2)^{-4}\epsilon^{11}$ |
| | | $q+q\to B^*+\bar B+qq$ | $(p_\perp^2)^{-8}\epsilon^7$ |
| | | $q+(qq)\to\bar B+B^*+B^*$ | $(p_\perp^2)^{-10}\epsilon^5$ |

PHYSICAL REVIEW D VOLUME 10, NUMBER 9 1 NOVEMBER 1974

# Unified description of inclusive and exclusive reactions at all momentum transfers*

R. Blankenbecler and S. J. Brodsky

TABLE I

Scaling Predictions for $E\, d\sigma/d^3p = C\, p_T^{-n} (1-x_T)^F$

| Large $p_T$ Process | Leading CIM Subprocess | Predicted | Observed (CP)[3] |
|---|---|---|---|
| | | n//F | n//F |
| $pp \to \pi^+ X$ | $qM \to q\pi^+$ | 8//9 | 8.5//8.8 |
| $\pi^-$ | $qM \to q\pi^-$ | 8//9 | 8.9//9.7 |
| $K^+$ | $qM \to qK^+$ | 8//9 | 8.4//8.8 |
| $K^-$ | $qM \to qK^-$ | 8//13 | 8.9//11.7 |
| | $q\bar{q} \to K^+K^-$ | 8//11 | |
| $pp \to pX$ | $q(qq) \to Mp$ | 12//5 | 11.7//6.8 |
| | $qB \to qp$ | 12//7 | |
| $pp \to \bar{p}X$ | $q\bar{q} \to B\bar{p}$ | 12//11 | 8.8//14.2 |
| | $qM \to qM$ | 8//15 | |
| $\pi p \to \pi X$ | $q\bar{q} \to M\pi$ | 8//5 | |
| | $qM \to q\pi$ | 8//7 | |
| | $q(qq) \to B\pi$ | 12//3 | |
| | $\pi q \to \pi q$ | 8//3 | |

# Which the energy range is interesting?

## NN-interactions and SPIN problems ($p_T$~ 2 GeV/c anomaly and the diquark nucleon component)

# pp -> pp ($90^0$ c.m.s.)

C.W. Akerlof et al., Phys.Rev., vol.159, N5, 1138-1149, 1967

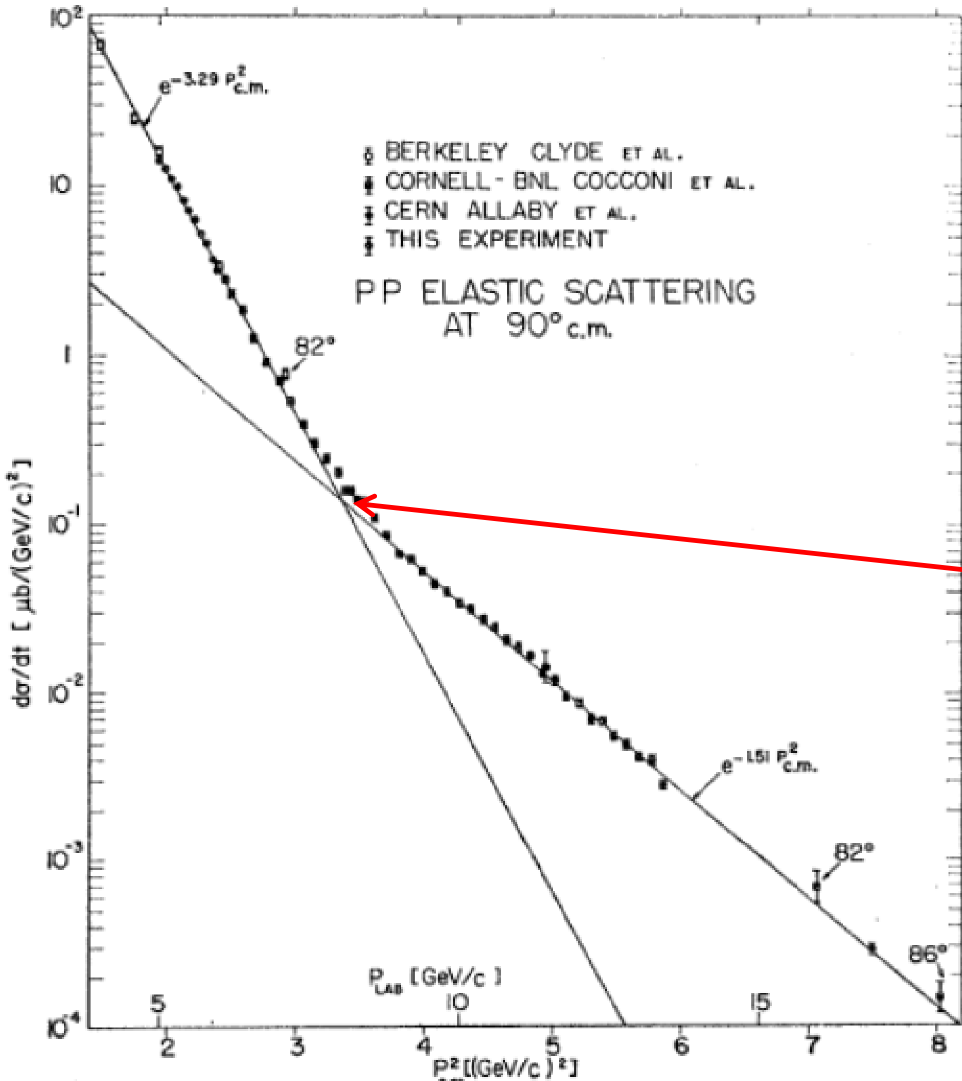


$p_T$ ~ 2 GeV/c

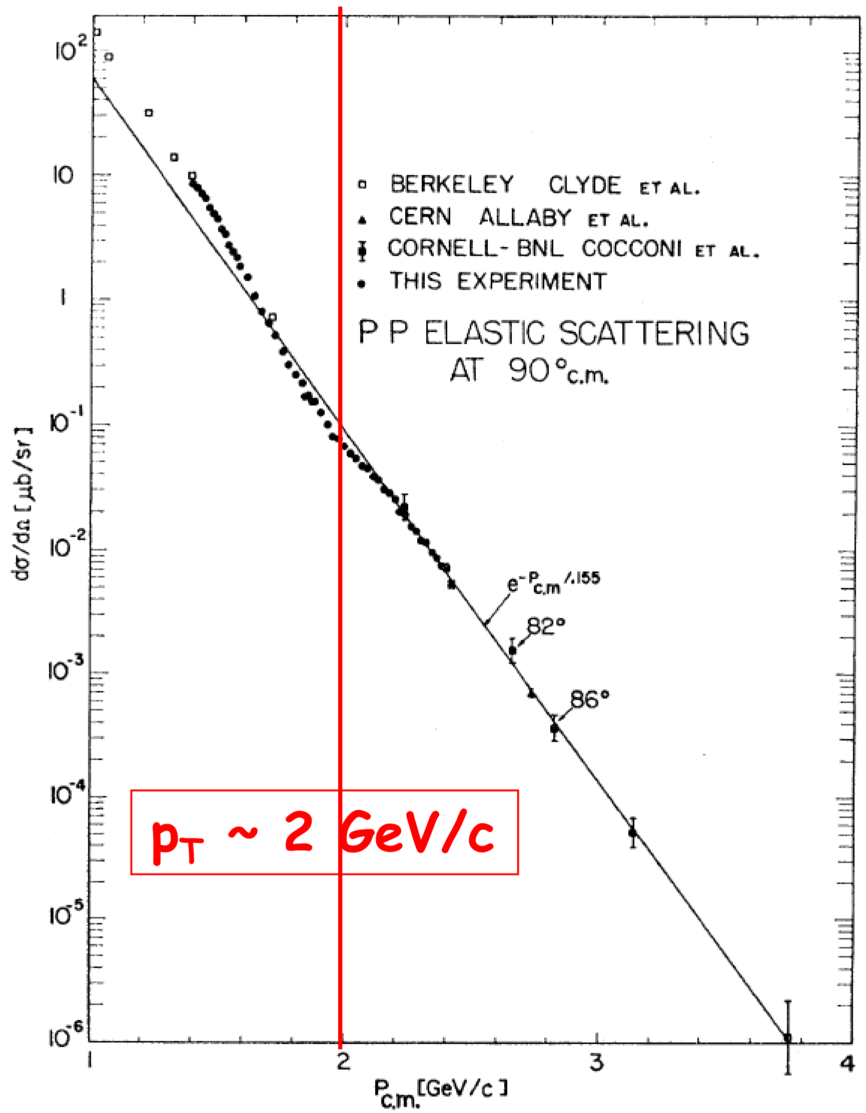


FIG. 9. Plot of $d\sigma/dt$ versus $\beta^2 P_\perp^2$ for all high-energy proton-proton elastic scattering. Other data (Refs. 13, 20, 22, 23), are also plotted. The lines drawn are straight line fits to the data.

## Cross-sections at 90 degrees

$p\,\bar{p}$

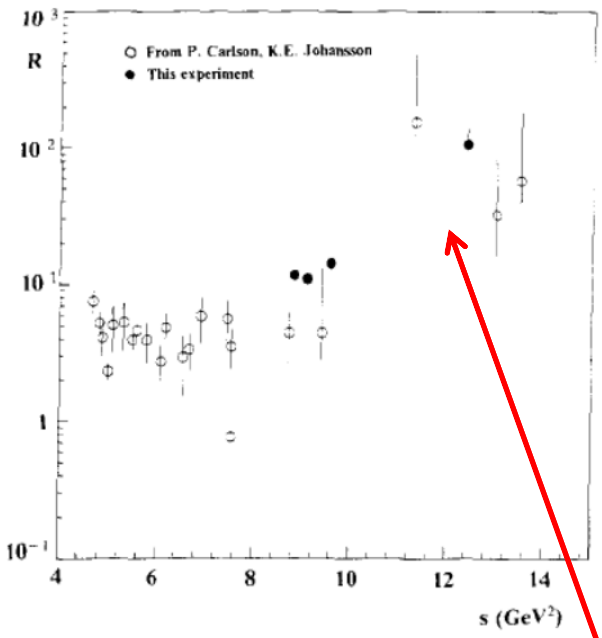


$$R = \frac{\sigma(pp \to pp)}{\sigma(\bar{p}p \to \bar{p}p)}(90^o\,c.m.)$$

$p_T$ ~ 2 GeV/c

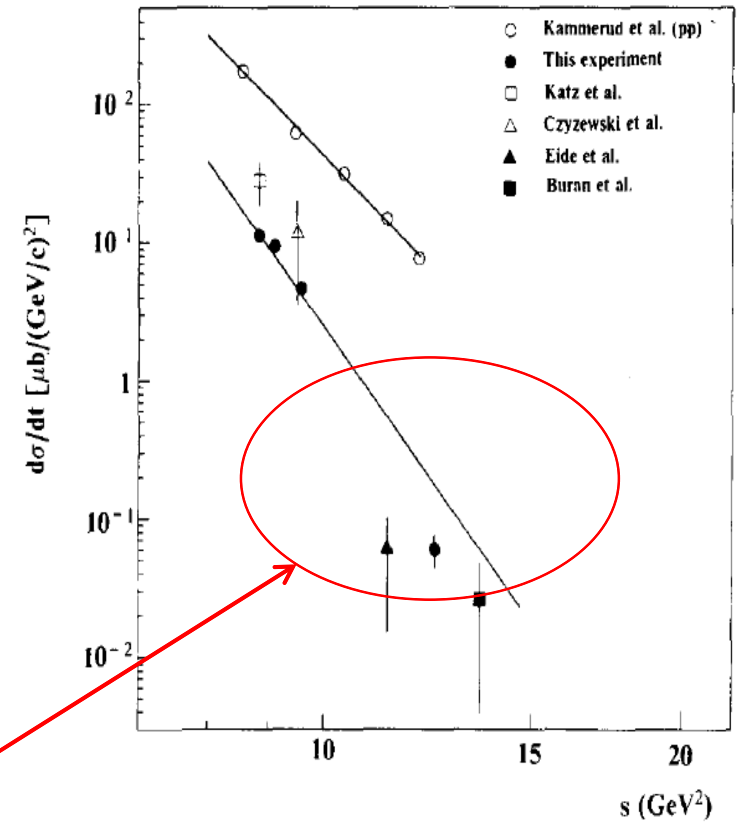


Fig. 3. The $p\bar{p}$ and pp elastic differential cross sections at 90° CM as function of the square of the CM energy, $s$. Open circles are pp data from ref. [6]. These data fit well to the drawn curve proportional to $s^{-9}$. The remaining points are $p\bar{p}$ data. Shaded from this experiment. Otherwise from ref. [7] (open square), ref. [8] (open triangle) ref. [9] (shaded triangle) and ref. [10] (shaded square). The lower curve is an $s^{-n}$ fit to four data points of this experiment, neglecting systematic errors. One obtains $n = 12.3 \pm 0.2$, but evidently the data do not seem to follow this kind of a power law.

C. Baglin et al., Phys.Lett. B, vol.225, N3, 296-300, 1989

Phys.Rev. C83 (2011) 054606
Carlos Granados and Misak Sargsian

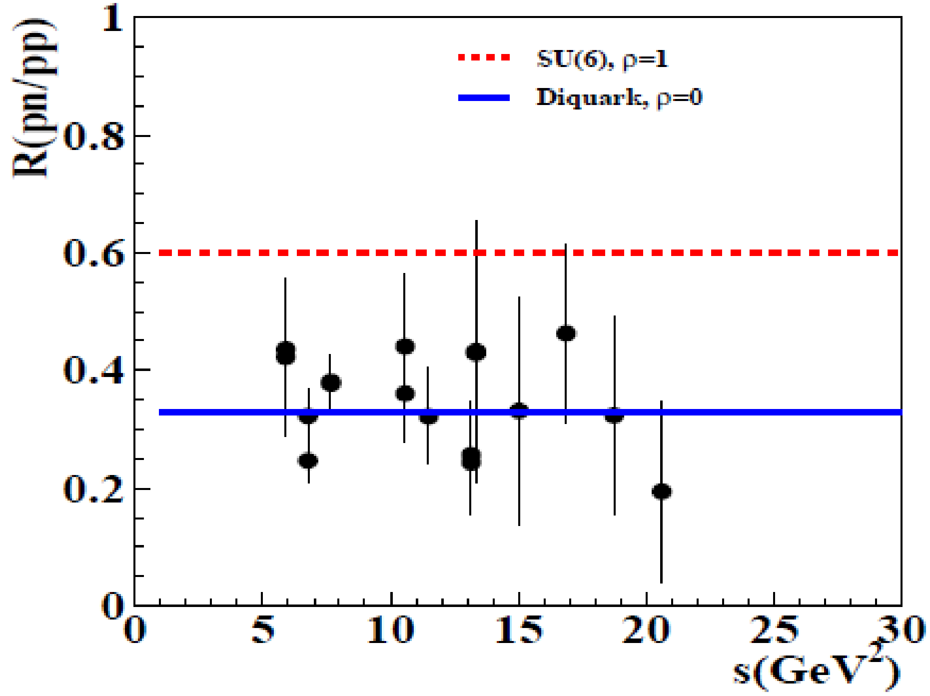


FIG. 2: (Color online) Ratio of the $pn \to pn$ to $pp \to pp$ elastic differential cross sections as a function of $s$ at $\theta^N_{c.m.} = 90^0$.

# SPIN physics and isotopic problem

Alan Krisch

# Answer to Questions by Profs. Weisskopf & Bethe

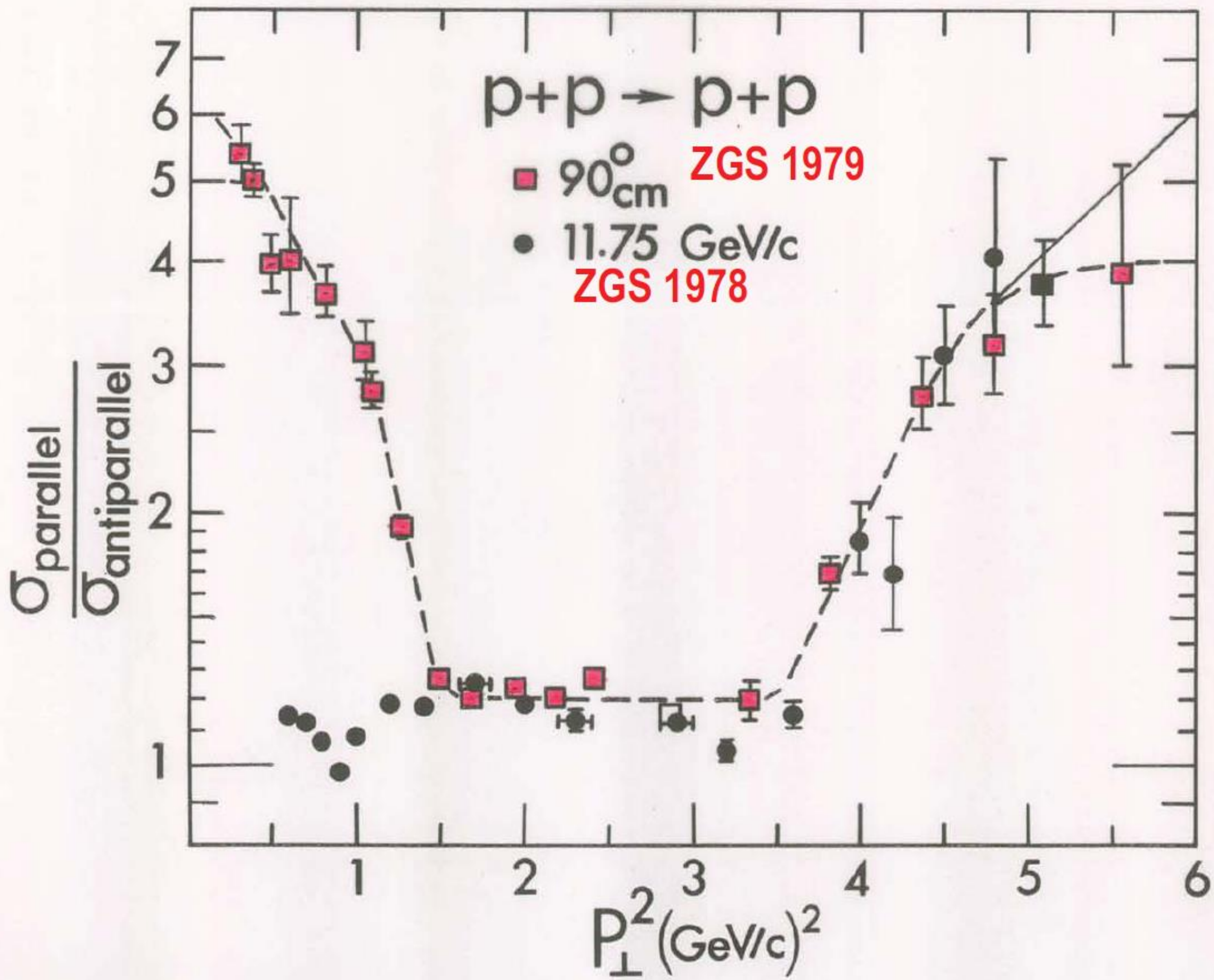

VOLUME 43, NUMBER 14 PHYSICAL REVIEW LETTERS 1 OCTOBER 1979

## Spin-Spin Forces in 6-GeV/c Neutron-Proton Elastic Scattering

D. G. Crabb, P. H. Hansen, A. D. Krisch, T. Shima, and K. M. Terwilliger
*Randall Laboratory of Physics, The University of Michigan, Ann Arbor, Michigan 48109*

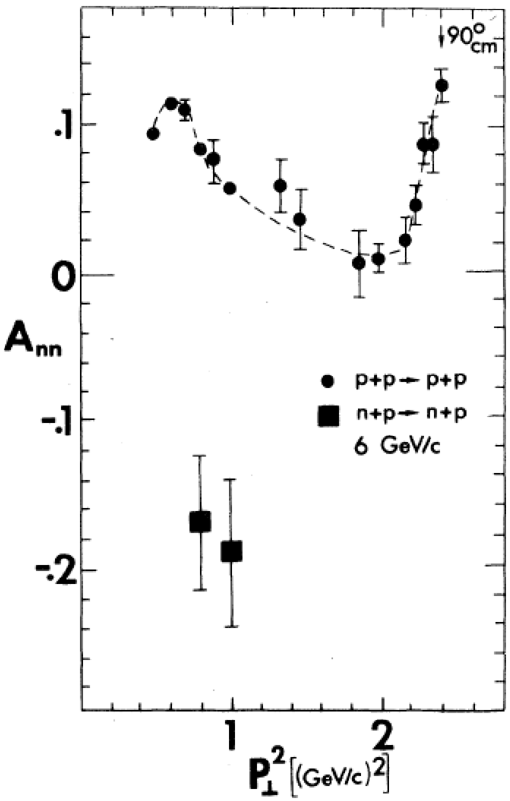


FIG. 2. The spin-spin correlation parameter, $A_{nn}$, for pure-initial-spin-state nucleon-nucleon elastic scattering at 6 GeV/$c$ is plotted against the square of the transverse momentum. The proton-proton and neutron-proton data are quite different.

This large negative $A_{nn}$ for $n$-$p$ elastic scattering is quite unexpected. No theoretical models predicted this effect, although a very recent constituent-interchange model[12] predicts $A_{nn} = -44\%$. This may support the suggestion that large spin effects are related to the composite nature of the nucleon.[12,13] An earlier Regge-model prediction[14] is inconsistent with our data. It seems somewhat surprising that $A_{nn}$ is so large at a $P_\perp^2$ of only 1 (GeV/$c$)$^2$.

[12]G. R. Farrar, S. Gottlieb, D. Sivers, and G. H. Thomas, Phys. Rev. D 20, 202 (1979).

# INCLUSIVE HYPERON POLARIZATION

Alan Krisch

**Devlin, Pondrum, Bunce, Heller *et al.* 1976-80**

Fermilab 400 GeV p+p -> Lambda ----

Plot by Heller ~1980

with KEK & ISR data

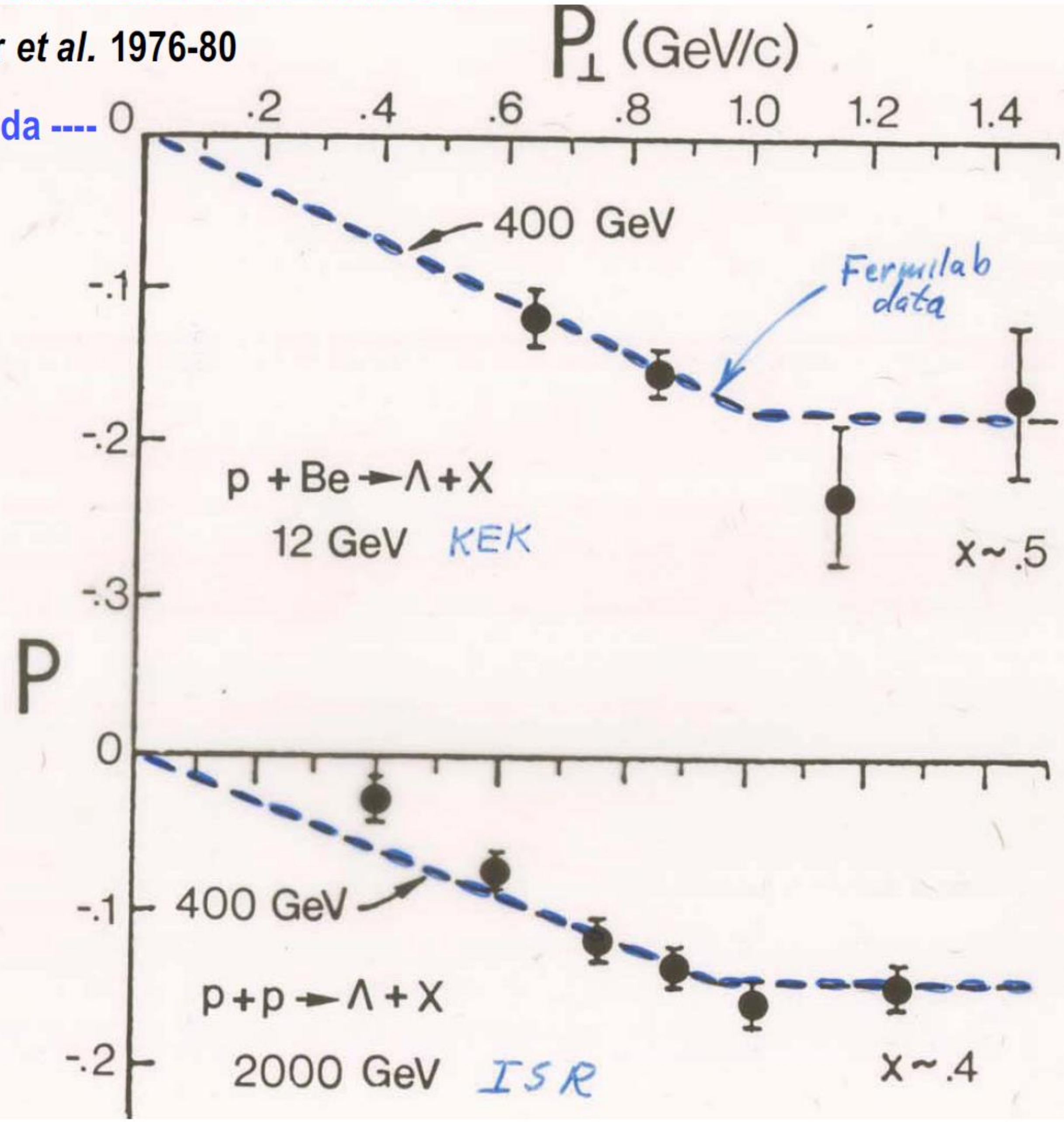


## P ~ 15-20 %

## QCD says P ~ 0

# pA - and AA - interactions

# Color Transparency

arXiv:1208.3668v1 [nucl-th] 17 Aug 2012

Gerald A. Miller

*Physics Department, Univ. of Washington, Seattle, Wa. 98195-1560, USA*

**Abstract.** Color transparency is the vanishing of nuclear initial or final state interactions involving specific reactions. The reasons for believing that color transparency might be a natural consequence of QCD are reviewed. The main impetus for this talk is recent experimental progress, and this is reviewed briefly.

The basic idea is that some times a hadron is in a color-neutral point-like configuration PLC. If such undergoes a coherent reaction, in which one sums gluon emission amplitudes to calculate the scattering amplitude, the PLC does not interact with the surrounding media. A PLC is not absorbed by the nucleus. The nucleus casts no shadow. This is a kind of quantum mechanical invisibility.

Progress in Particle and Nuclear Physics 69 (2013) 1–27

Review

## Color transparency: Past, present and future

D. Dutta[a,*], K. Hafidi[b], M. Strikman[c]

# Color(nuclear) transparency in $90^0$ c.m. quasielastic *A*(*p*,2*p*) reactions

*The incident momenta varied from 5.9 to 14.4 GeV/c, corresponding to $4.8 < Q^2 < 12.7\ (GeV/c)^2$.*

$$T = \frac{\frac{d\sigma}{dt}(p + "p" \rightarrow p + p)}{Z\frac{d\sigma}{dt}(p + p \rightarrow p + p)}$$

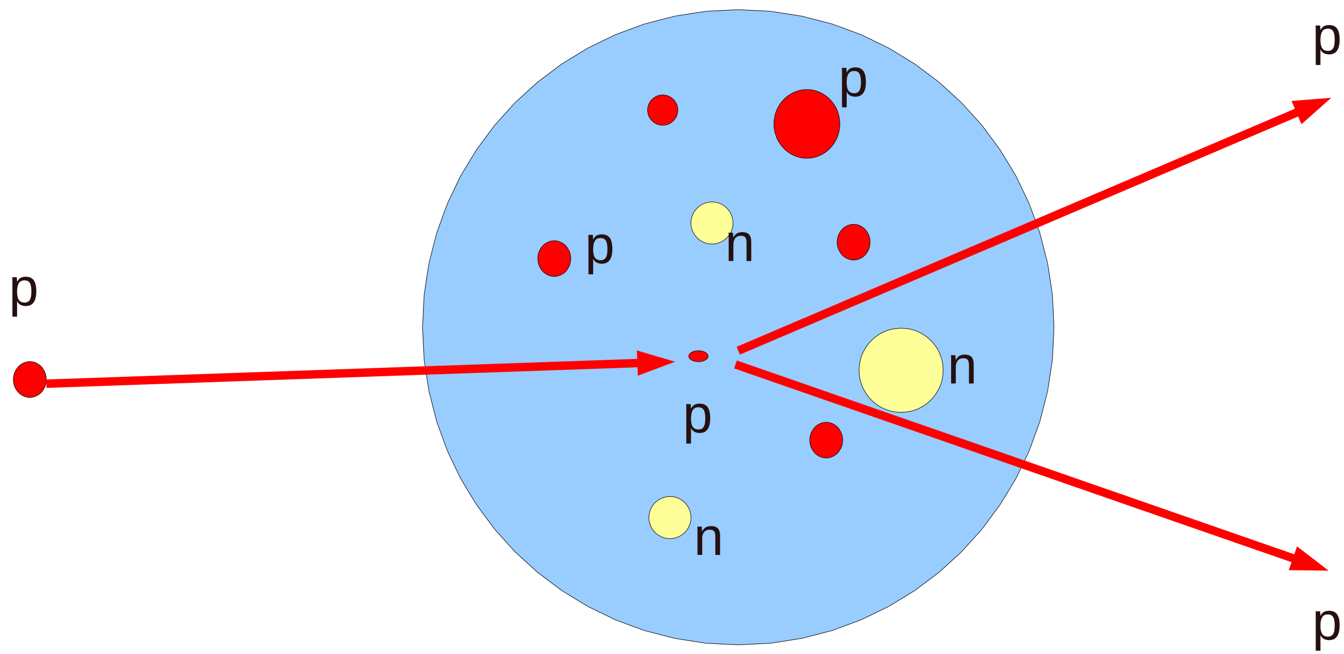

# Energy Dependence of Nuclear Transparency in C($p$,2$p$) Scattering

A. Leksanov,[5] J. Alster,[1] G. Asryan,[3,2] Y. Averichev,[8] D. Barton,[3] V. Baturin,[5,4] N. Bukhtoyarova,[3,4] A. Carroll,[3] S. Heppelmann,[5] T. Kawabata,[6] Y. Makdisi,[3] A. Malki,[1] E. Minina,[5] I. Navon,[1] H. Nicholson,[7] A. Ogawa,[5] Yu. Panebratsev,[8] E. Piasetzky,[1] A. Schetkovsky,[5,4] S. Shimanskiy,[8] A. Tang,[9] J. W. Watson,[9] H. Yoshida,[6] and D. Zhalov[5]

[1]*School of Physics and Astronomy, Sackler Faculty of Exact Sciences, Tel Aviv University, Ramat Aviv 69978, Isra*
[2]*Yerevan Physics Institute, Yerevan 375036, Armenia*
[3]*Collider-Accelerator Department, Brookhaven National Laboratory, Upton, New York, 11973*
[4]*Petersburg Nuclear Physics Institute, Gatchina, St. Petersburg 188350, Russia*
[5]*Physics Department, Pennsylvania State University, University Park, Pennsylvania 16801*
[6]*Department of Physics, Kyoto University, Sakyoku, Kyoto, 606-8502, Japan*
[7]*Department of Physics, Mount Holyoke College, South Hadley, Massachusetts 01075*
[8]*J.I.N.R., Dubna, Moscow 141980, Russia*
[9]*Department of Physics, Kent State University, Kent, Ohio 44242*
(Received 20 April 2001; published 6 November 2001)

The transparency of carbon for $(p,2p)$ quasielastic events was measured at beam momenta ranging from 5.9 to 14.5 GeV/$c$ at 90° c.m. The four-momentum transfer squared ($Q^2$) ranged from 4.7 to 12.7 (GeV/$c$)$^2$. We present the observed beam momentum dependence of the ratio of the carbon to hydrogen cross sections. We also apply a model for the nuclear momentum distribution of carbon to obtain the nuclear transparency. We find a sharp rise in transparency as the beam momentum is increased to 9 GeV/$c$ and a reduction to approximately the Glauber level at higher energies.

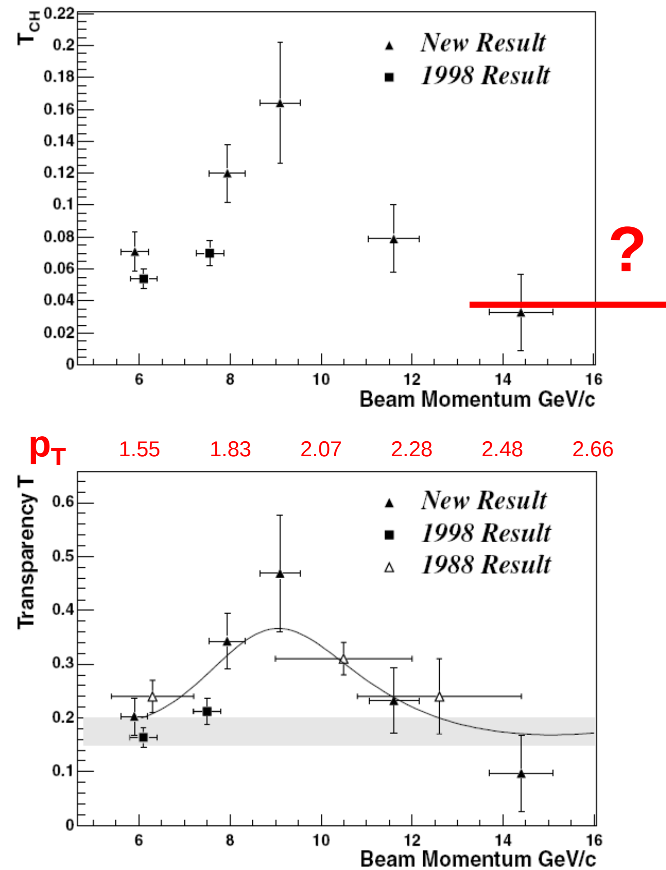


$$T_{CH} = T \int d\alpha \int d^2\vec{P}_{FT}\, n(\alpha, \vec{P}_{FT})\, \frac{(\frac{d\sigma}{dt})_{pp}(s(\alpha))}{(\frac{d\sigma}{dt})_{pp}(s_0)}$$

$$\alpha \equiv A\,\frac{(E_F - P_{Fz})}{M_A} \simeq 1 - \frac{P_{Fz}}{m_p}$$

FIG. 2. Top: The transparency ratio $T_{CH}$ as a function of the beam momentum for both the present result and two points from the 1998 publication [3]. Bottom: The transparency $T$ versus beam momentum. The vertical errors shown here are all statistical errors, which dominate for these measurements. The horizontal errors reflect the $\alpha$ bin used. The shaded band represents the Glauber calculation for carbon [9]. The solid curve shows the shape $R^{-1}$ as defined in the text. The 1998 data cover the c.m. angular region from 86°–90°. For the new data, a similar angular region is covered as is discussed in the text. The 1988 data cover 81°–90° c.m.

**J.W. Cronin et al., Production of hadrons at large transverse momentum at 200, 300, and 400 GeV, Phys.Rev. D, v.11, N 11, 3105-3123 (1975)**

**$p_T$ ~ 2 GeV/c region**

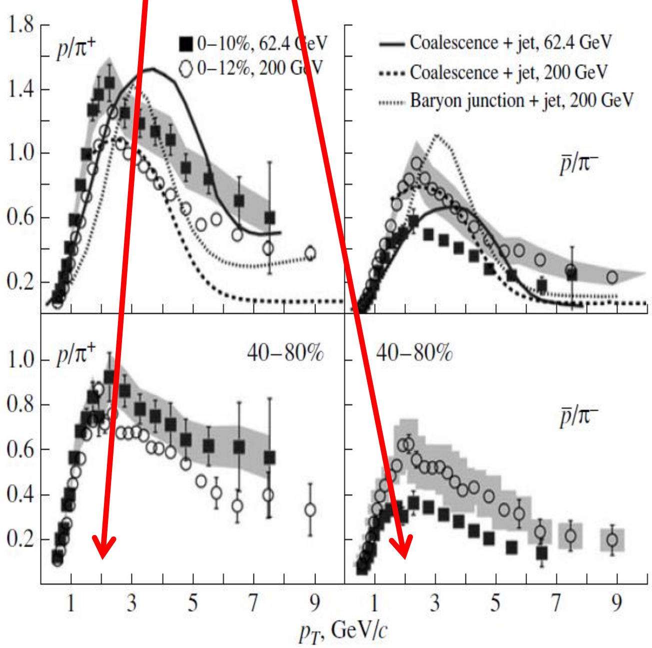


Fig. 3. [10] Ratio of the cross sections for the production of protons and charged pions as a function of the transverse momentum for various degrees of centrality and two beam energies of 62.4 and 200 GeV: (points) results of the STAR experiment and (curves) results of model calculations.

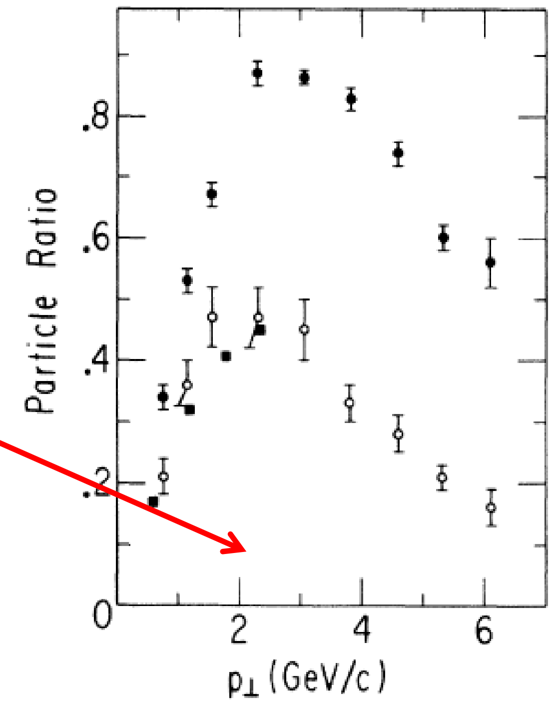


FIG. 20. Comparison of the cross-section ratio $p/\pi^+$ measured on tungsten at $\sqrt{s}=23.7$ GeV (closed circles), with that obtained by extrapolation to $A=1$ (open circles). Ratios obtained from the British-Scandinavian collabortion (Ref. 23) at $\sqrt{s}=23.4$ GeV are also plotted (closed squares).

**V.S. Pantuev *Physics of Atomic Nuclei, 2009, Vol. 72, No. 12, pp. 1971–1981***

# Baryon anomaly in Pb-Pb

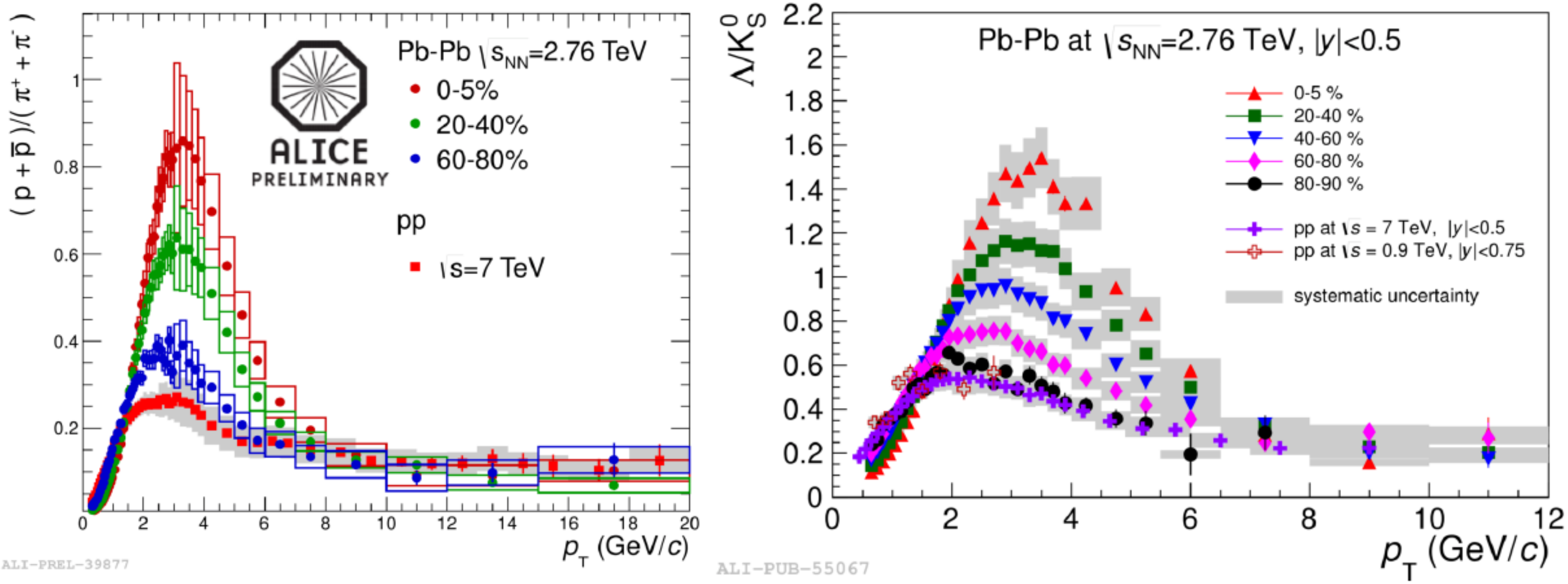


- Baryon to meson ratio increasing with centrality for $p_T$ < 8 GeV/c.
  - Enhancement at moderate $p_T$ is consistent with radial flow
  - May be explained by quark recombination from QGP (coalescence model)
- For $p_T$ > 8 GeV/c no dependence on centrality and collision system
  - Consistent with fragmentation in vacuum

# $p_T$~2 GeV/c anomaly at high energy (RHIC and LHC)

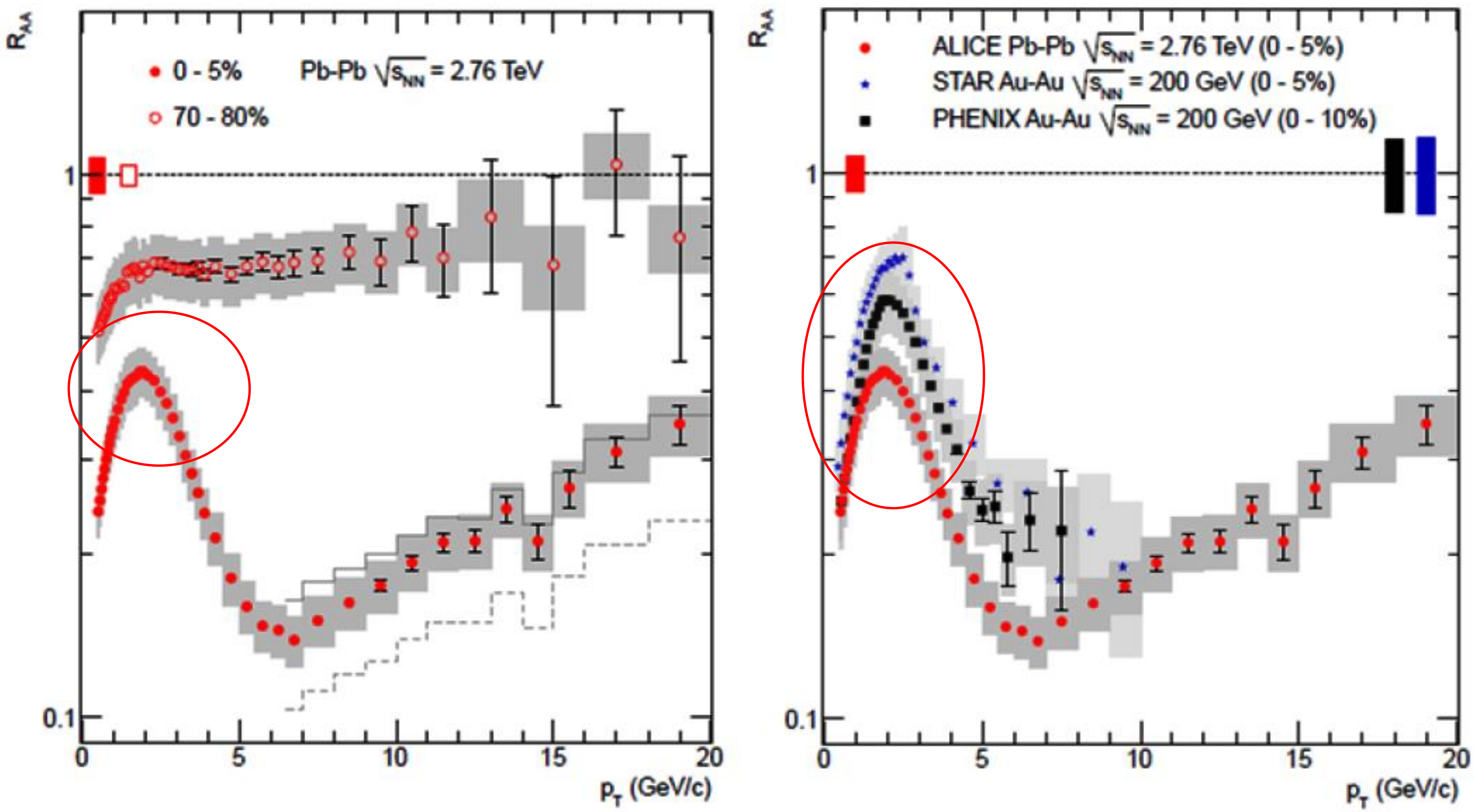

VOLUME 5, NUMBER 1 PHYSICAL REVIEW LETTERS JULY 1, 1960

MASS ANALYSIS OF THE SECONDARY PARTICLES PRODUCED BY THE 25-GEV PROTON BEAM OF THE CERN PROTON SYNCHROTRON

V. T. Cocconi,* T. Fazzini, G. Fidecaro, M. Legros,† N. H. Lipman, and A. W. Merrison
CERN, Geneva, Switzerland
(Received June 1, 1960)

We present here some results of a mass analysis of the secondary particles produced at 15.9° to the circulating beam in an aluminum target bombarded by 25-Gev protons in the CERN proton synchrotron.

D/p ratio

p/π ratio

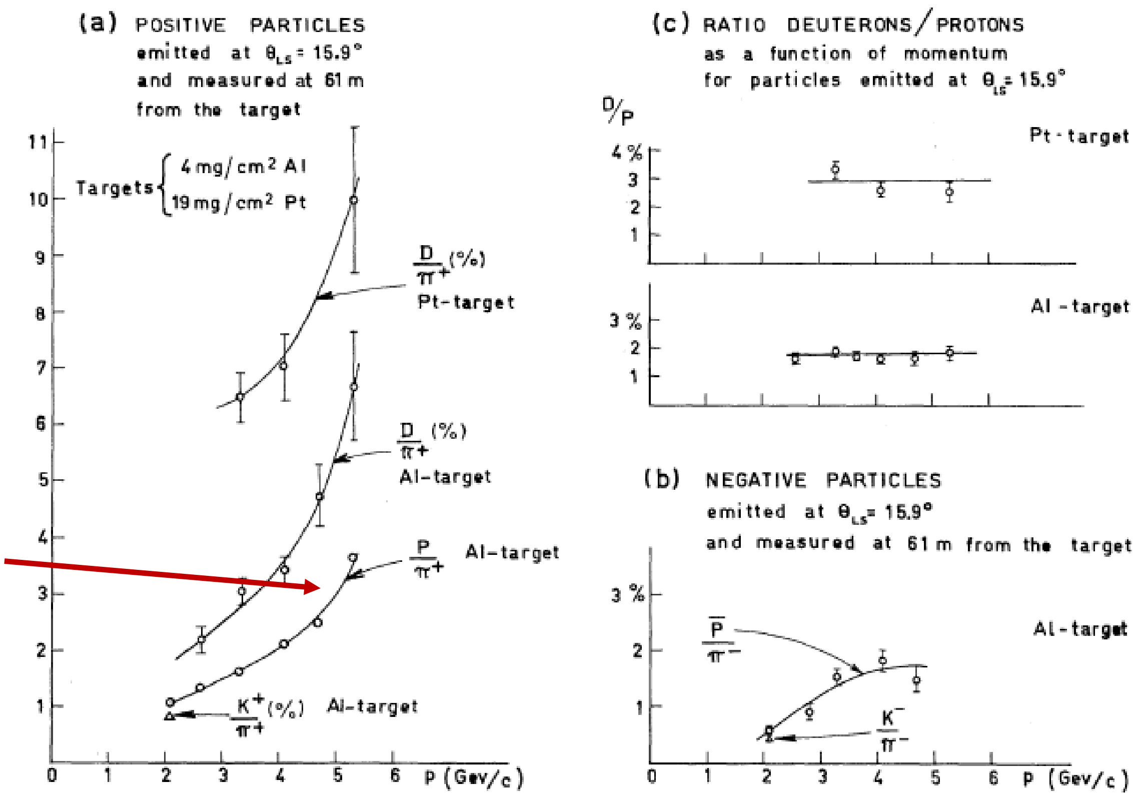

ЯДЕРНАЯ ФИЗИКА
JOURNAL OF NUCLEAR PHYSICS
т. 45, вып. 5, 1987

D/p ratio

# ОБРАЗОВАНИЕ ДЕЙТРОНОВ И АНТИДЕЙТРОНОВ С БОЛЬШИМИ $p_\perp$ В $pp$- И $pA$-СОУДАРЕНИЯХ ПРИ ЭНЕРГИИ 70 ГэВ

АБРАМОВ В. В., БАЛДИН Б. Ю., БУЗУЛУЦКОВ А. Ф., ВАСИЛЬЧЕНКО В. Г., ВОЛКОВ А. А., ГЛЕБОВ В. Ю., ДЫШКАНТ А. С., ЕВДОКИМОВ В. Н., ЕФИМОВ А. О., ЗМУШКО В. В., КРИНИЦЫН А. Н., КРЫШКИН В.И., МУТАФЯН М. И., ПОДСТАВКОВ В. М., РОНЖИН А. И., СУЛЯЕВ Р. М., ТУРЧАНОВИЧ Л. К.

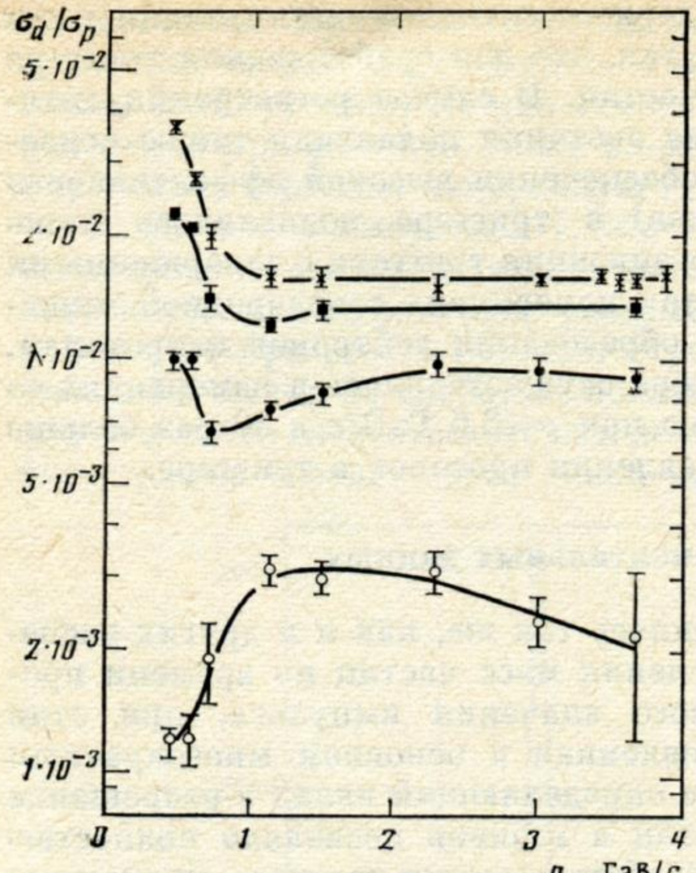


Рис. 3. Зависимость отношений сечений образования $\sigma_d/\sigma_p$ от $p_\perp$ в $pp$- и $pA$-взаимодействиях. Точки: ○ – $pp$, ● – $p$Be, ■ – $p$Cu, × – $p$Pb. Кривые проведены от руки

V.T. Kim

# DIQUARKS AND DYNAMICS OF LARGE-$P_\perp$ BARYON PRODUCTION

Modern Physics Letters A, Vol. 3, No. 9 (1988) 909–916



In the framework of a diquark model of the nucleon, the strong scaling violation of the $p/\pi^+$-ratio in the $pp$-collisions from $\sqrt{s} = 11.5$ GeV (IHEP, Serpukhov) to $\sqrt{s} = 23.4$ GeV (FNAL) and to $\sqrt{s} = 62$ GeV (CERN ISR) is described. A fairly good description of the magnitude of cross sections for single protons and for symmetric-proton-pairs with large-$p_\perp$ is obtained. In the model with the dominating scalar $(ud)$-diquark, the yield relation $\Lambda^0/p \simeq K^+/\pi^+$ is predicted.

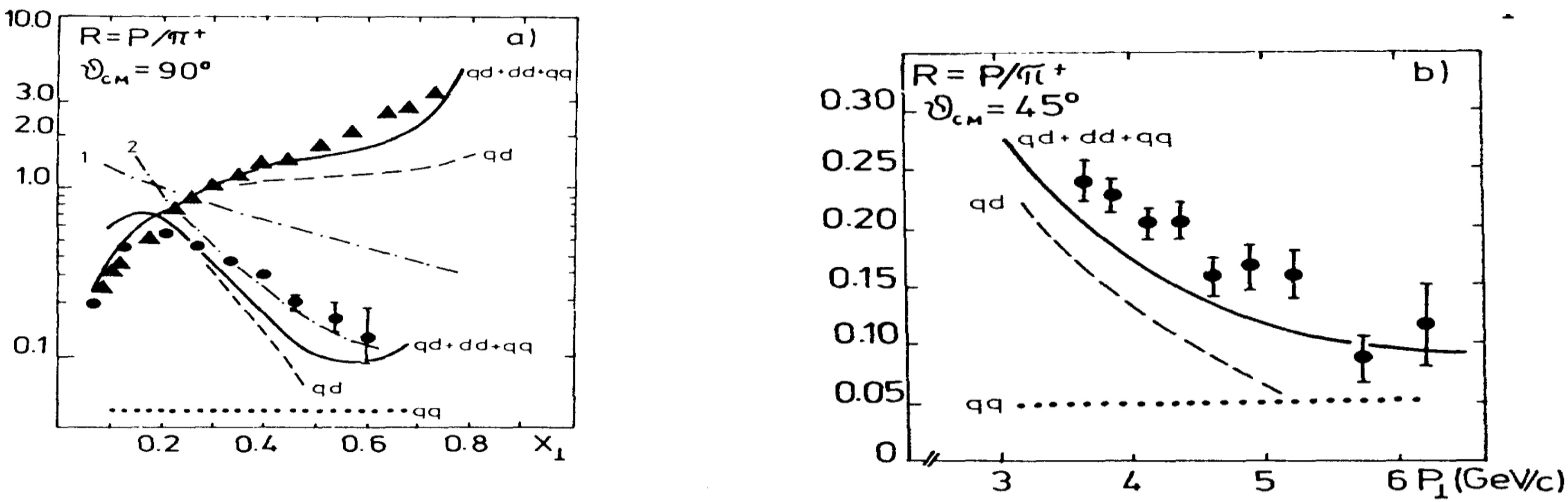


Fig. 1. $R = p/\pi^+$ is the particle yield ratio in the $pp$-collisions.
a) $\vartheta_{CM} = 90°$: • the FNAL data[1] at $\sqrt{s} = 23.4$ GeV ($E = 300$ GeV); ▲ the IHEP (Serpukhov) data[2] at $\sqrt{s} = 11.5$ GeV ($E = 70$ GeV).
b) $\vartheta_{CM} = 45°$: • the CERN ISR data[3] at $\sqrt{s} = 62$ GeV ($E \simeq 1900$ GeV).
The dotted curve shows the contribution of the $qq$-subprocess, the dashed one shows the contribution of the $qd$-subprocess. The total contribution of the $qq$-, $qd$- and $dd$-subprocesses is denoted by the solid lines. The dashed-dotted curves show the calculations with the diquark function $G_d^N(x) \sim (1-x)/x$ at 70 GeV (curve 1) and at 300 GeV (curve 2).

3) The dominating contribution to the $(ud)$-diquark scattering in the nucleon collisions must lead to a high yield of large-$p_\perp$ $\Lambda^0$-hyperons. In particular, the following relation for the particle yields in the nucleon collisions

$$\frac{\Lambda^0}{p} \simeq \frac{K^+}{\pi^+} \left( \text{or } \frac{\Lambda^0}{K^+} \simeq \frac{p}{\pi^+} \right) \tag{9}$$

must be observed, i.e. the scaling violation in the $\Lambda^0/K^+$-ratio must be the same as in the $p/\pi^+$-ratio. The deviation of the $\Lambda^0/K^+$ from the $p/\pi^+$ by the constant may be explained by the $(uu)$-diquark contribution in the $p/\pi^+$-ratio. Different behaviour of both $\Lambda^0/K^+$ and $p/\pi^+$ with $x_\perp$ $(p_\perp)$ may indicate the contribution of other higher twists.[11]

4) Anomalously high yield of large-$p_\perp$ deuterons in the $pp$-collisions[22] also may give the evidence for the diquarks.[23] A simultaneous double quark-diquark scattering may lead to the production of the large-$p_\perp$ deuteron as well as to the production of the $H$-dihyperon.[23]

END

# "The high $p_T$ physics at PANDA(FAIR) and SPD(NICA)"

*Shimanskiy S.S. (JINR)*

# HIGH $p_T$ ISSUES

1. Diquark properties.
2. Nature of the spin effects.
3. Exotic states and flavor universality.
4. …

5. Nature of CsDBM and CT.
6. $\Lambda$N – hypernuclei.
7. Subthreshold J/$\Psi$ production.
8. …

# CUMULATIVE PROCESSES

SOVIET PHYSICS JETP VOLUME 6 (33), NUMBER 5 MAY, 1958

# *ON THE FLUCTUATIONS OF NUCLEAR MATTER*

D. I. BLOKHINTSEV

Joint Institute for Nuclear Research

Submitted to JETP editor July 1, 1957

J. Exptl. Theoret. Phys. (U.S.S.R.) 33, 1295-1299 (November, 1957)

It is shown that the production of energetic nuclear fragments in collisions with fast nucleons can be interpreted in terms of collisions of the incoming nucleon with the density fluctuations of the nuclear matter.

## 1. INTRODUCTION

THE motion of nucleons in nuclei can result in short-lived tight nucleon clusters, in other words, in density fluctuations of nuclear matter. Since such clusters are relatively far removed from the other nucleons of the nucleus, they become atomic nuclei of lower mass in a state of fluctuating compression.

In their study of the scattering of 675-Mev protons by light nuclei, Meshcheriakov and coworkers[1,2] observed recently certain effects which confirm the existence of such fluctuations, at least for the simplest nucleon-pair fluctuations, which lead to the formation of a compressed deuteron.

Schroeder L.S. et al. // Phys. Rev. Lett. 1979. V. 43, n. 24. P. 1787

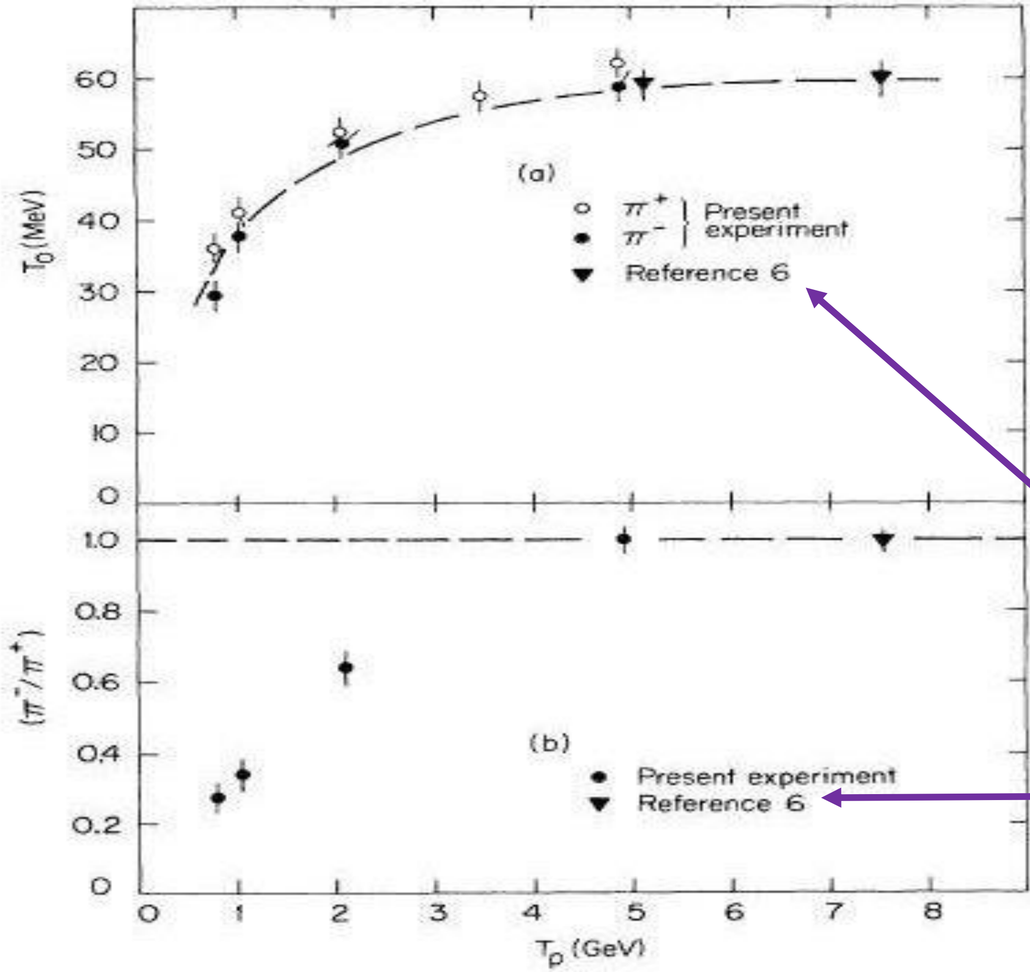


A.M. Baldin et al., Yad.Fiz., 20, 1975, p.1201

FIG. 1. Energy dependence of (a) $T_0$ parameter for pions, and (b) the $\pi^-/\pi^+$ ratio at 180° obtained by integrating each spectra up to 100 MeV for $p$-Cu collisions from 0.8 to 4.89 GeV. The dashed curve in both cases refers to the predictions of the "effective-target" model (Refs. 3 and 4).

Volume 67B, number 1 PHYSICS LETTERS 14 March 1977

ТЕОРИЯ

# LARGE MOMENTUM PION PRODUCTION IN PROTON NUCLEUS COLLISIONS AND THE IDEA OF "FLUCTUONS" IN NUCLEI

V.V. BUROV
*The Moscow State University, Moscow, USSR*

and

V.K. LUKYANOV and A.I. TITOV
*Joint Institute for Nuclear Research, Dubna, USSR*

Received 27 January 1977

It is shown that in proton-nucleus collisions, the production of pions with large momenta can be explained by the assumption of the existence of nuclear density fluctuations ("fluctuons") at short distances of the nucleon core radius order, with the mass of several nucleons.

The purpose of this note is to realize the idea [4] that the cumulative effect is connected largely with a suggestion on the existence in nuclei of the so-called fluctuons. Earlier fluctuons were proposed [7] in order to understand the nature of the "deuteron peak" in the pA-scattering cross section at large momentum transfers [8] and also to interpret the pd-scattering

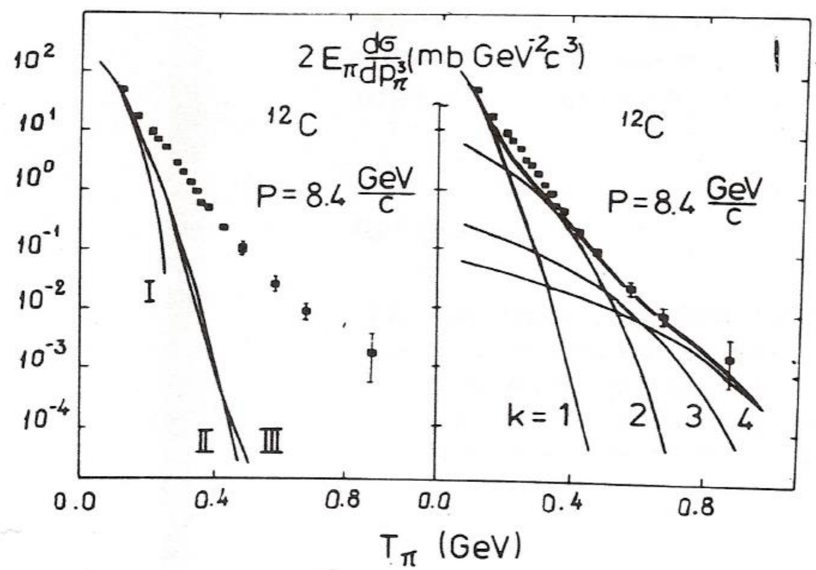


Fig. 1. (a) Calculations of the invariant pion production cross section for $^{12}$C: I – for the free proton target; II – with fermi motion; III – the relativization effect. (b) The contributions of separate fluctuons with mass $M_k = km_p$ where $k$ is the order of cumulativity.

cross section [9]. Compressional fluctuations of ma $M_k = km_p$ of nucleons in the small volume $V_\xi = \frac{4}{3}\pi r$ where $r_\xi$ is the fluctuon radius were assumed.

PHYSICAL REVIEW C VOLUME 45, NUMBER 4 APRIL 1992

# Nuclear structure functions at $x > 1$

B. W. Filippone, R. D. McKeown, R. G. Milner,* and D. H. Potterveld†
*Kellogg Radiation Laboratory, California Institute of Technology, Pasadena, California 91125*

D. B. Day, J. S. McCarthy, Z. Meziani,‡ R. Minehardt, R. Sealock, and S. T. Thornton
*Institute of Nuclear and Particle Physics and Department of Physics, University of Virginia, Charlottesville, Virginia 22901*

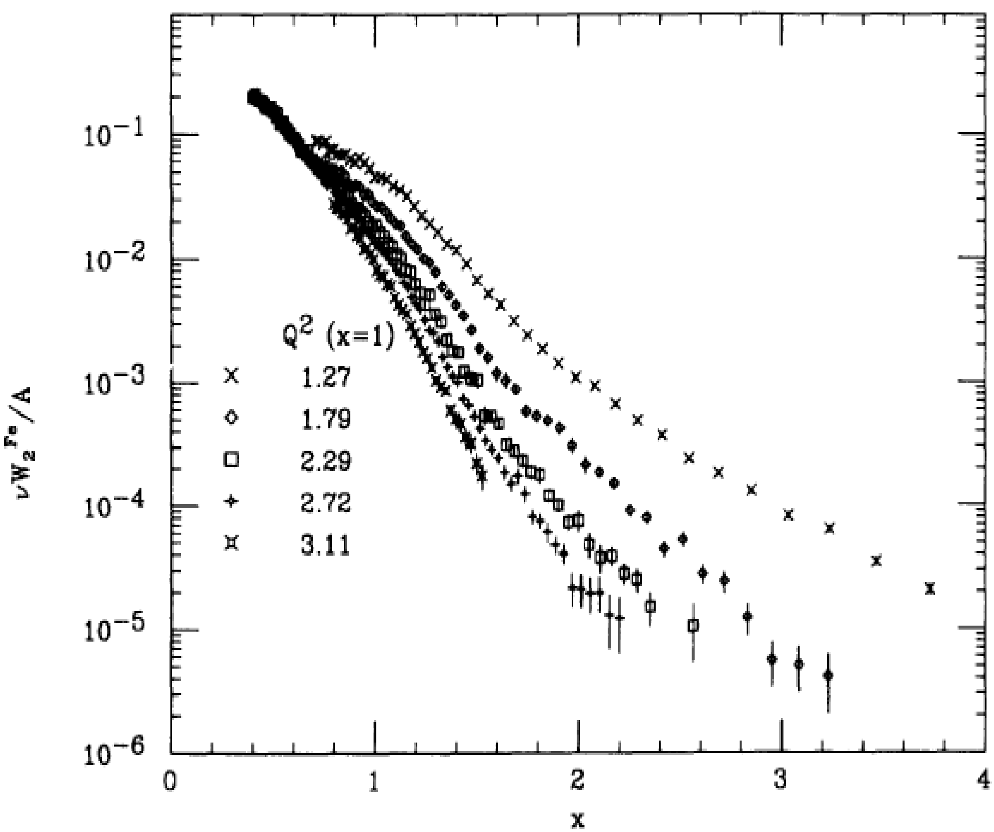


41

FIG. 1. Measured structure function per nucleon for Fe vs $x$. The $Q^2$ value at $x=1$ is also listed for the different kinematics.

Phys.Rev.Lett. 96 (2006) 082501

# Measurement of 2- and 3-Nucleon Short Range Correlation Probabilities in Nuclei

K.S. Egiyan,[1] N.B. Dashyan,[1] M.M. Sargsian,[10] M.I. Strikman,[28] L.B. Weinstein,[27] G. Adams,[30] P. Ambrozewicz,[10] M. Anghinolfi,[16] B. Asavapibhop,[22] G. Asryan,[1] H. Avakian,[34] H. Baghdasaryan,[27] N. Baillie,[38] J.P. Ball,[2]

$$r(A, {}^3\mathrm{He}) = \frac{A(2\sigma_{ep} + \sigma_{en})}{3(Z\sigma_{ep} + N\sigma_{en})} \frac{3\mathcal{Y}(A)}{A\mathcal{Y}({}^3\mathrm{He})} C^A_{\mathrm{rad}}, \qquad (2)$$

where $Z$ and $N$ are the number of protons and neutrons in nucleus $A$, $\sigma_{eN}$ is the electron-nucleon cross section, $\mathcal{Y}$ is the normalized yield in a given $(Q^2, x_B)$ bin [30] and $C^A_{\mathrm{rad}}$ is the ratio of the radiative correction factors for $A$ and ${}^3$He ($C^A_{\mathrm{rad}} = 0.95$ and $0.92$ for ${}^{12}$C and ${}^{56}$Fe respectively). In our $Q^2$ range, the elementary cross section correction factor $\frac{A(2\sigma_{ep}+\sigma_{en})}{3(Z\sigma_{ep}+N\sigma_{en})}$ is $1.14 \pm 0.02$ for C and ${}^4$He and $1.18 \pm 0.02$ for ${}^{56}$Fe. Fig. 1 shows the resulting ratios integrated over $1.4 < Q^2 < 2.6$ GeV$^2$.

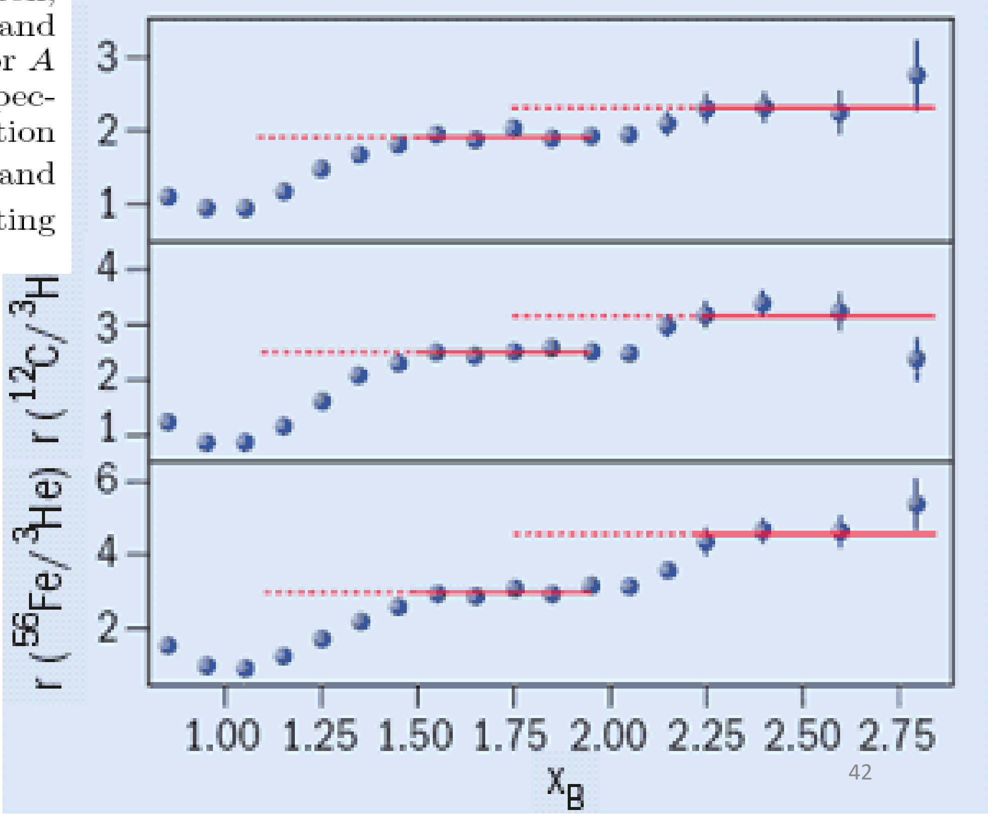

Having these data, we know almost full (≈99%) nucleonic picture of nuclei with $A \leq 56$

| Fractions / Nucleus | Single particle (%) | 2N SRC (%) | 3N SRC (%) |
|---|---|---|---|
| $^{56}$Fe | **76** ± 0.2 ± 4.7 | **23.0** ± 0.2 ± 4.7 | **0.79** ± 0.03 ± 0.25 |
| $^{12}$C | **80** ± 02 ± 4.1 | **19.3** ± 0.2 ± 4.1 | **0.55** ± 0.03 ± 0.18 |
| $^{4}$He | **86** ± 0.2 ± 3.3 | **15.4** ± 0.2 ± 3.3 | **0.42** ± 0.02 ± 0.14 |
| $^{3}$He | **92** ± 1.6 | **8.0** ± 1.6 | **0.18** ± 0.06 |
| $^{2}$H | **96** ± 0.8 | **4.0** ± 0.8 | ----- |

Using the published data on (p,2p+n) [PRL,90 (2003) 042301] estimate the isotopic composition of 2N SRC in $^{12}$C

$a_{pp}(^{12}C) \approx$ 4 ± 2 %

$a_{2N}(^{12}C) \approx 20 \pm 0.2 \pm 4.1$ % → $a_{pn}(^{12}C) \approx 12 \pm 4$ %

$a_{nn}(^{12}C) \approx$ 4 ± 2 %



43

# $^{12}C$ - structure

## RNP – program at JINR

V.V.Burov, V.K.Lukyanov, A.I.Titov, PLB, 67, 46(1977)

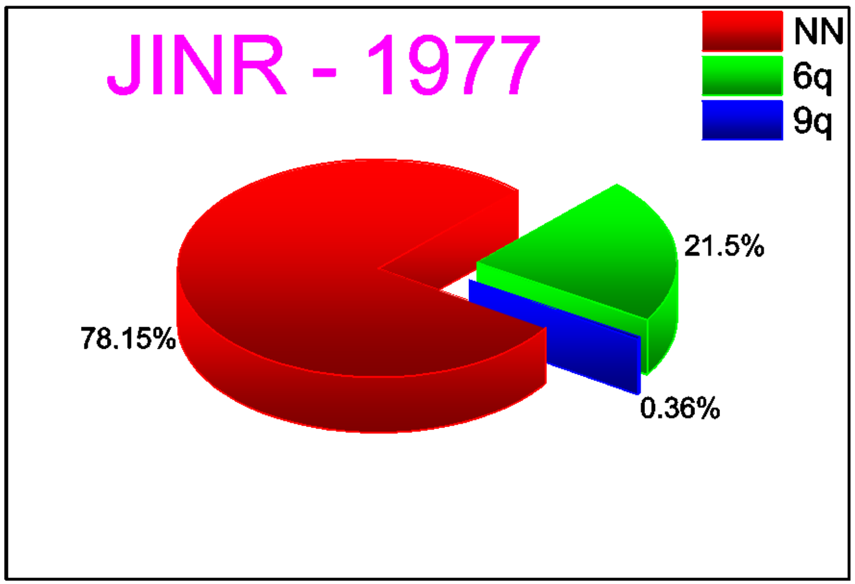


## eA – program at JLab

R.Subedi et al., Science 320 (2008) 1476-1478
e-Print: arXiv:0908.1514 [nucl-ex]

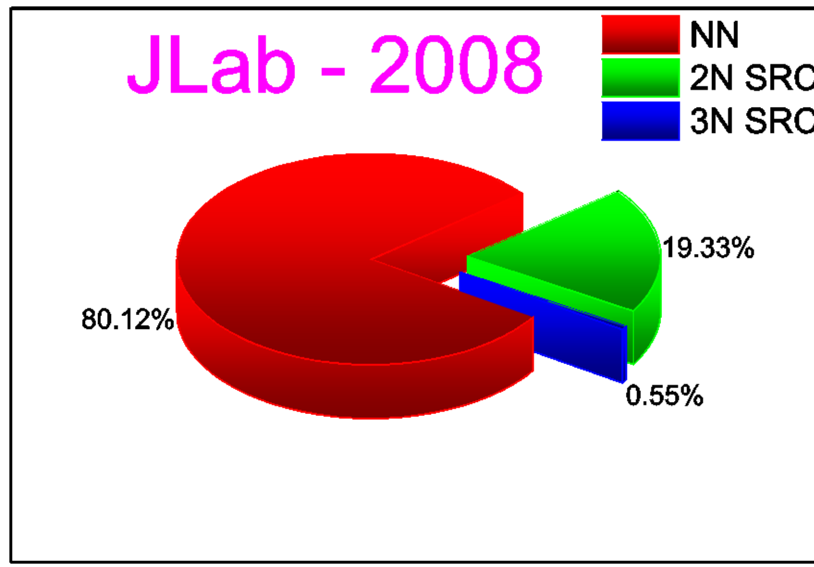


44

## “Flucton”

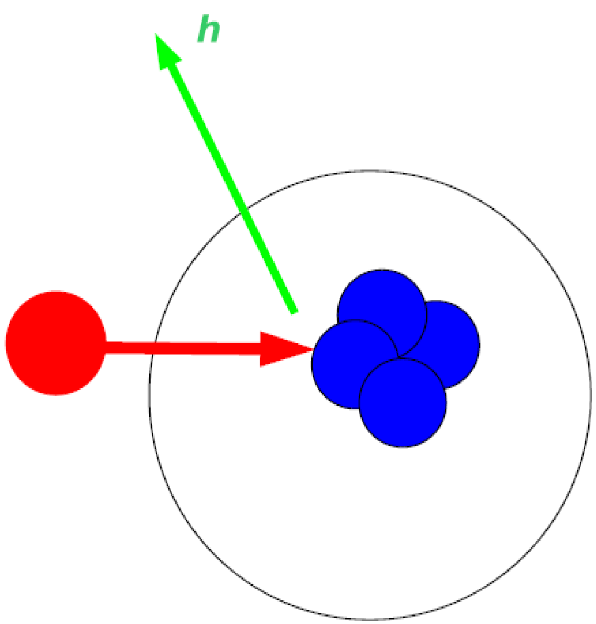


## “SRC”

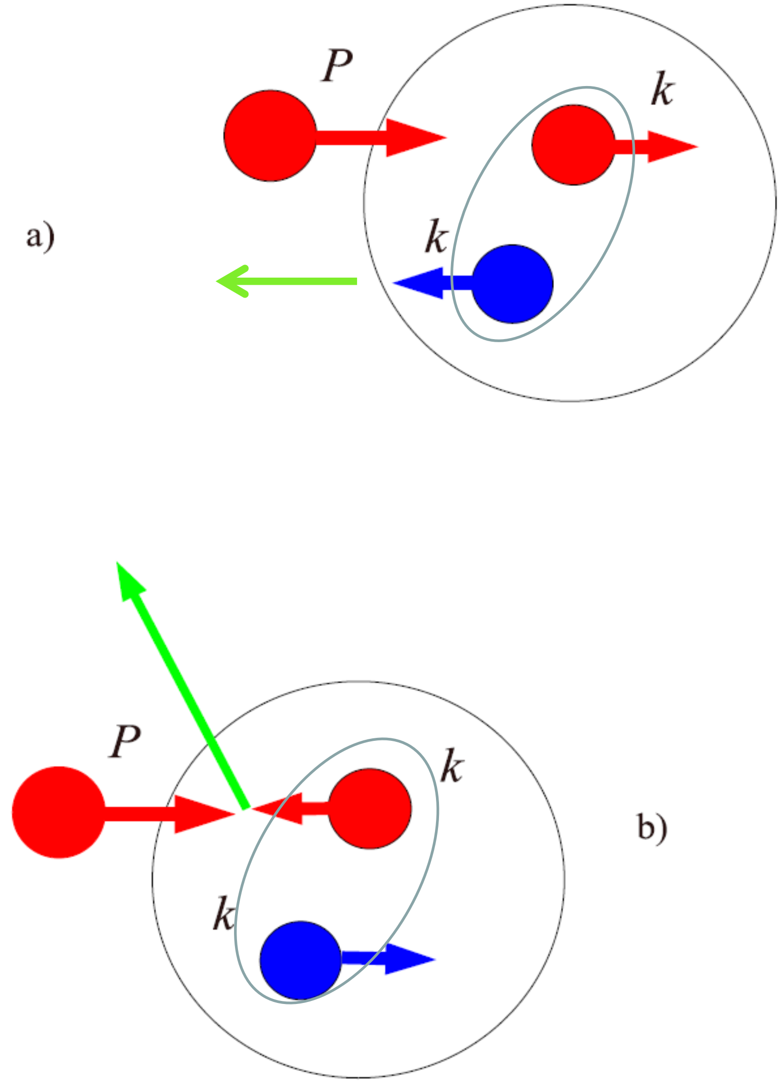

# Knot out cold dense nuclear configurations

SRC configuration

Multiquark configuration

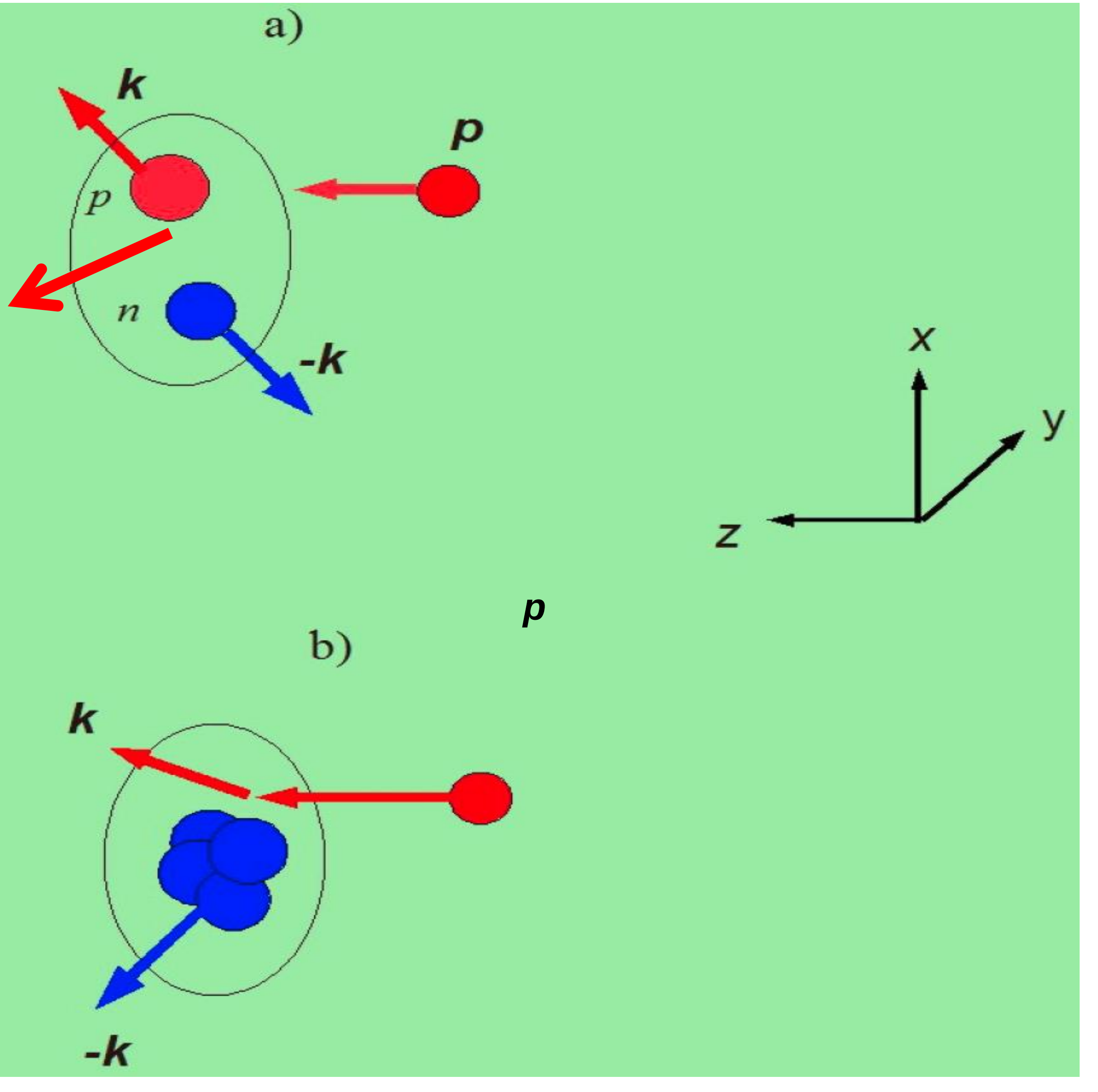

N.N. Antonov et al., *JETP Letters*, Vol.101, No.10, pp.670-673(2015)

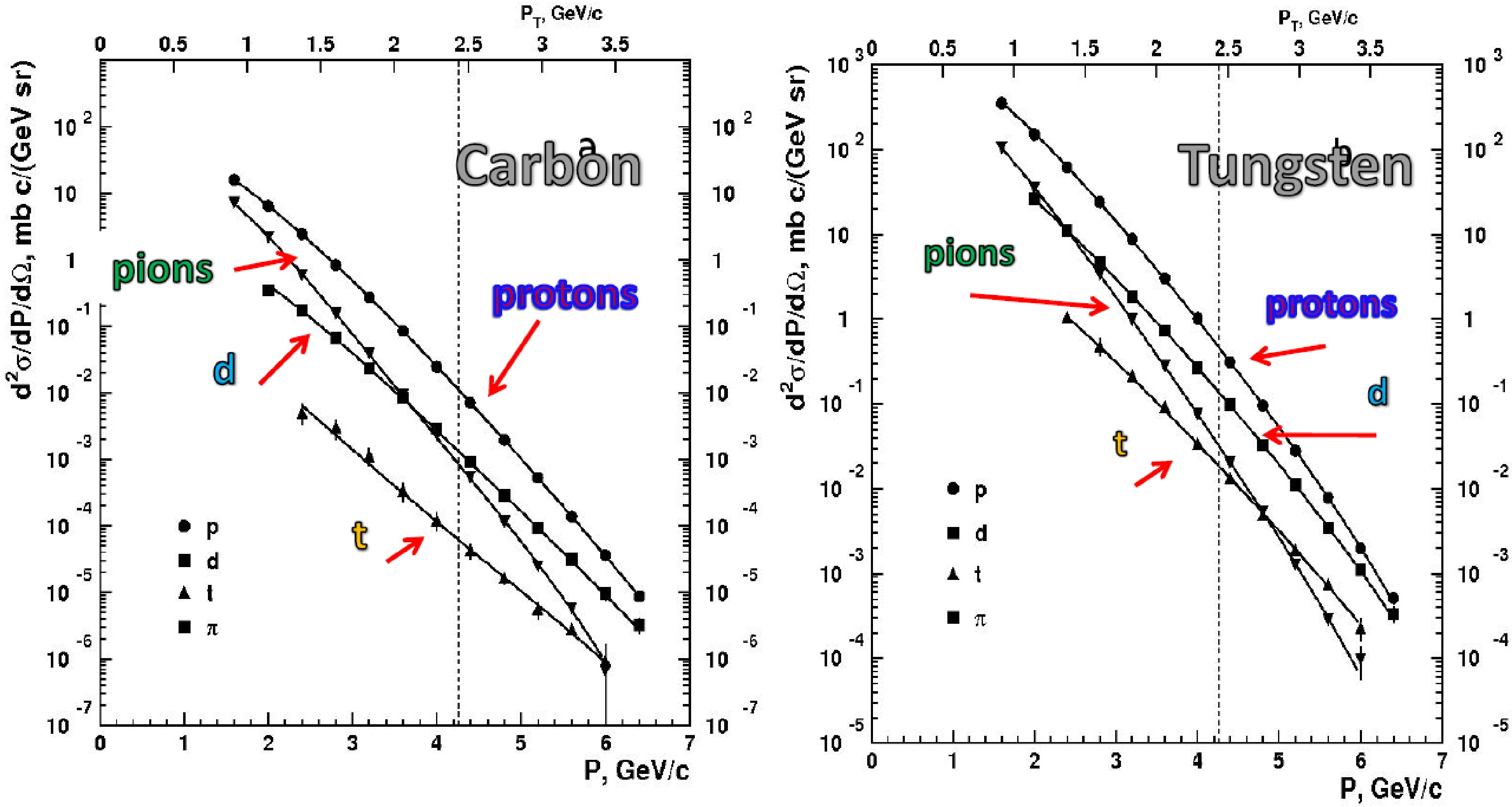


***Invariant function found for positive pion, proton, deuteron and triton.***
*The vertical dashed lines indicate the kinematical limit for elastic nucleon–nucleon scattering. The upper horizontal scale shows values of the transverse momentum* $p_T$ .

N.N. Antonov et al., JETP Letters, Vol.101, No.10, pp.670-673(2015)

# Average baryon number <B>

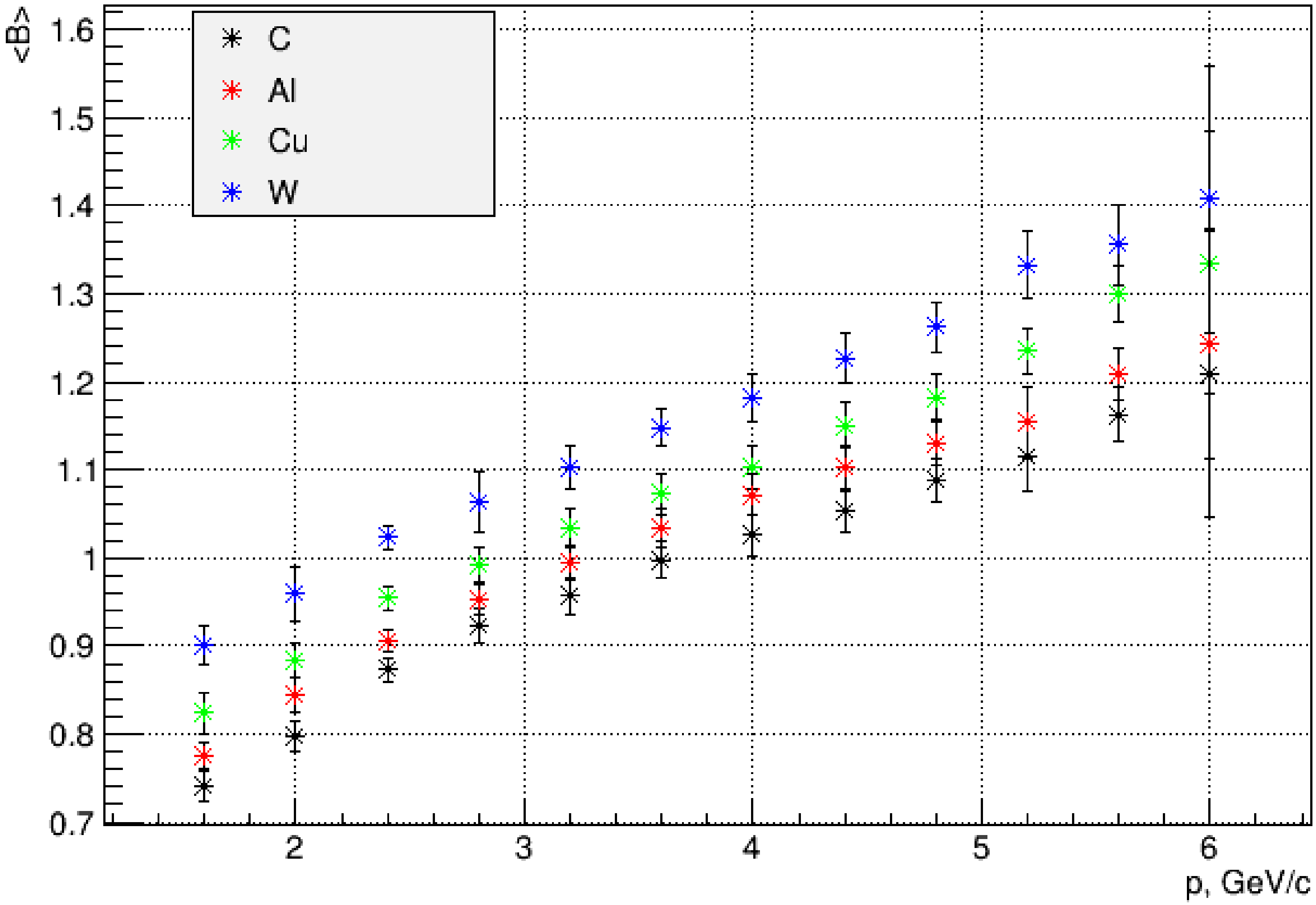

PHYSICAL REVIEW VOLUME 126, NUMBER 5 JUNE 1, 1962

# Particle Production at Large Angles by 30- and 33-Bev Protons Incident on Aluminum and Beryllium*

V. L. Fitch, S. L. Meyer,† and P. A. Piroué
*Palmer Physical Laboratory, Princeton University, Princeton, New Jersey*
(Received February 12, 1962)

A mass analysis has been made of the relatively low momentum particles emitted from Al and Be targets when struck by 30- and 33-Bev protons. Measurements were made at 90°, 45°, and $13\frac{1}{4}$° relative to the direction of the Brookhaven AGS proton beam. Magnetic deflection and time-of-flight technique were used to determine the mass of the particles.

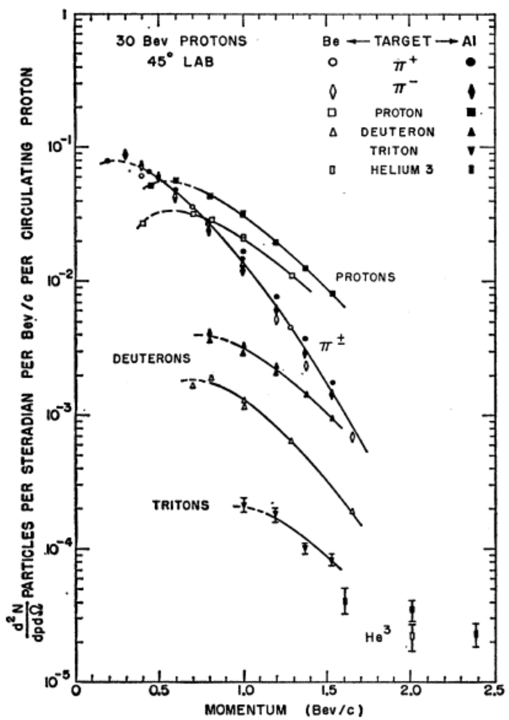


Fig. 3. Momentum spectra of particles emitted at 45° from aluminum and beryllium targets when struck by 30-Bev protons. Tritons from Be were not measured. For general remarks refer to Fig. 2 caption.

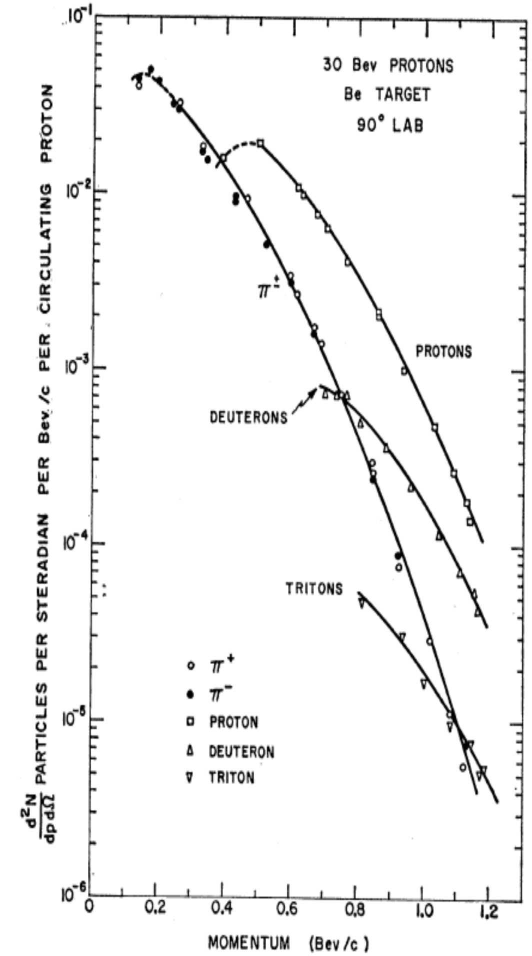


Fig. 2. Momentum spectrum of particles emitted at 90° from a beryllium target struck by 30-Bev protons. The ordinate is the number of particles produced at the target per steradian per Bev/$c$ per circulating proton. The dashed portions of the curves indicate regions where the corrections due to multiple scattering exceed 15%. At the time these data were taken no effort was made to detect $He^3$.

ISSN 0021-3640, JETP Letters, 2016, Vol. 104, No. 10, pp. 662–665. © Pleiades Publishing, Inc., 2016.
Original Russian Text © N.N. Antonov, A.A. Baldin, V.A. Viktorov, V.A. Gapienko, G.S. Gapienko, V.N. Gres', M.A. Ilyushin, V.A. Korotkov, A.I. Mysnik, A.F. Prudkoglyad, A.A. Semak, V.I. Terekhov, V.Ya. Uglekov, M.N. Ukhanov, B.V. Chuiko, S.S. Shimanskii, 2016, published in Pis'ma v Zhurnal Eksperimental'noi i Teoreticheskoi Fiziki, 2016, Vol. 104, No. 10, pp. 678–681.

FIELDS, PARTICLES, AND NUCLEI

# Knockout of Deuterons and Tritons with Large Transverse Momenta in *pA* Collisions Involving 50-GeV Protons

N. N. Antonov[a], A. A. Baldin[b], V. A. Viktorov[a], V. A. Gapienko[a, *], G. S. Gapienko[a], V. N. Gres'[a], M. A. Ilyushin [a], V. A. Korotkov[a], A. I. Mysnik[a], A. F. Prudkoglyad[a], A. A. Semak[a], V. I. Terekhov[a], V. Ya. Uglekov[a], M. N. Ukhanov[a], B. V. Chuiko[a†], and S. S. Shimanskii[b]

$$\frac{E_d}{\sigma_{inel}}\frac{d^3\sigma_A}{dp_A^3} = B_A \times \left(\frac{E_p}{\sigma_{inel}}\frac{d^3\sigma_p}{dp_p^3}\right)^A$$

Mean values of the $B_2$ parameter

| Target | C | Al | Cu | W |
|---|---|---|---|---|
| $B_2 \times 10^2$, GeV$^2/c^3$ | $1.41 \pm 0.10$ | $1.56 \pm 0.08$ | $1.51 \pm 0.07$ | $1.41 \pm 0.06$ |

$B_2 \sim V^{-1}$ $B_3 \sim V^{-2})$

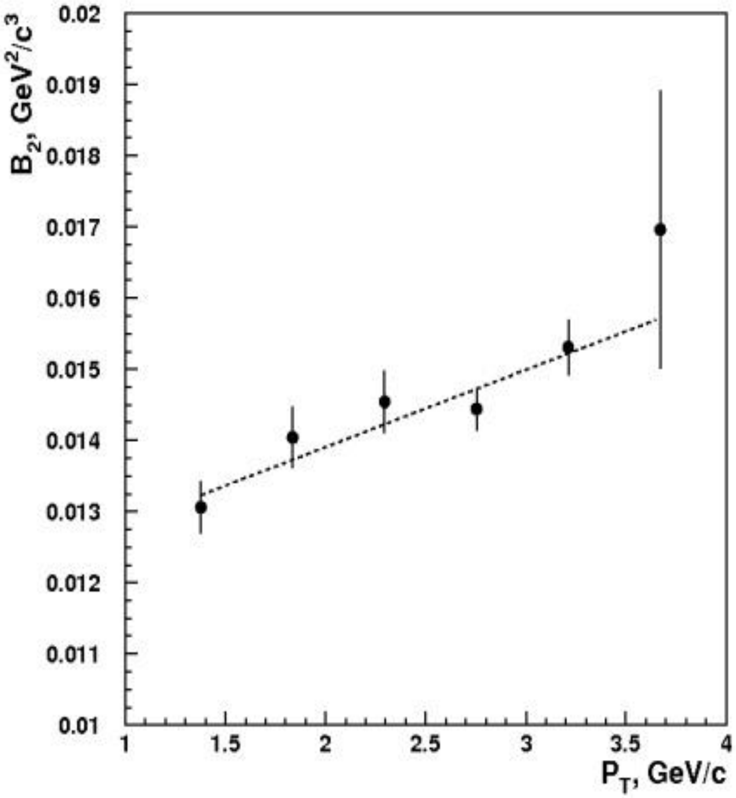


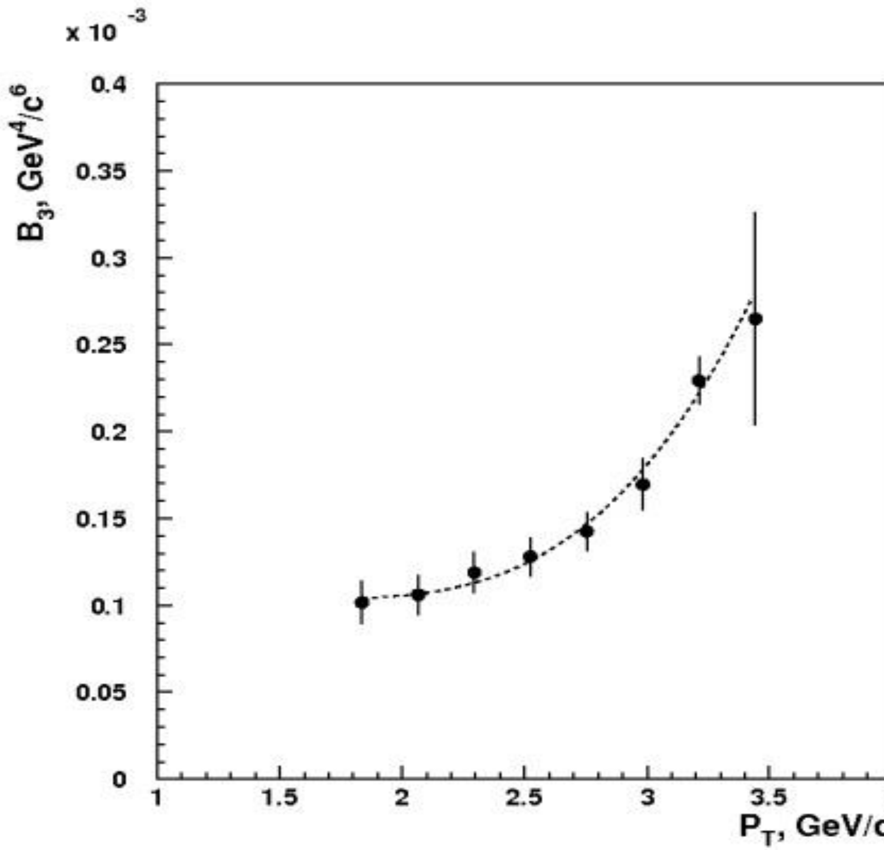

# CsDBM

1.Cold - exists inside ordinary nuclear matter as a quantum component of the wave function (with some probability and life time).

2. superDense - several nucleons can be in a volume less than the nucleon volume. The mass will be several nucleon masses. The small size means that the multinucleon(multiquark) configuration seeing as point like objects in processes with high transfer energy.

3. Baryonic Matter – enhancement of baryonic states and suppression of sea and gluon degrees of freedom (mesons and antiparticles production).

“New directions in science are launched by new tools much more often than by new concepts.

The effect of a concept-driven revolution is to explain old things in new ways.

The effect of a tool-driven revolution is to discover new things that have to be explained”

From Freeman Dyson ‘Imagined Worlds’

# PANDA Spectrometer

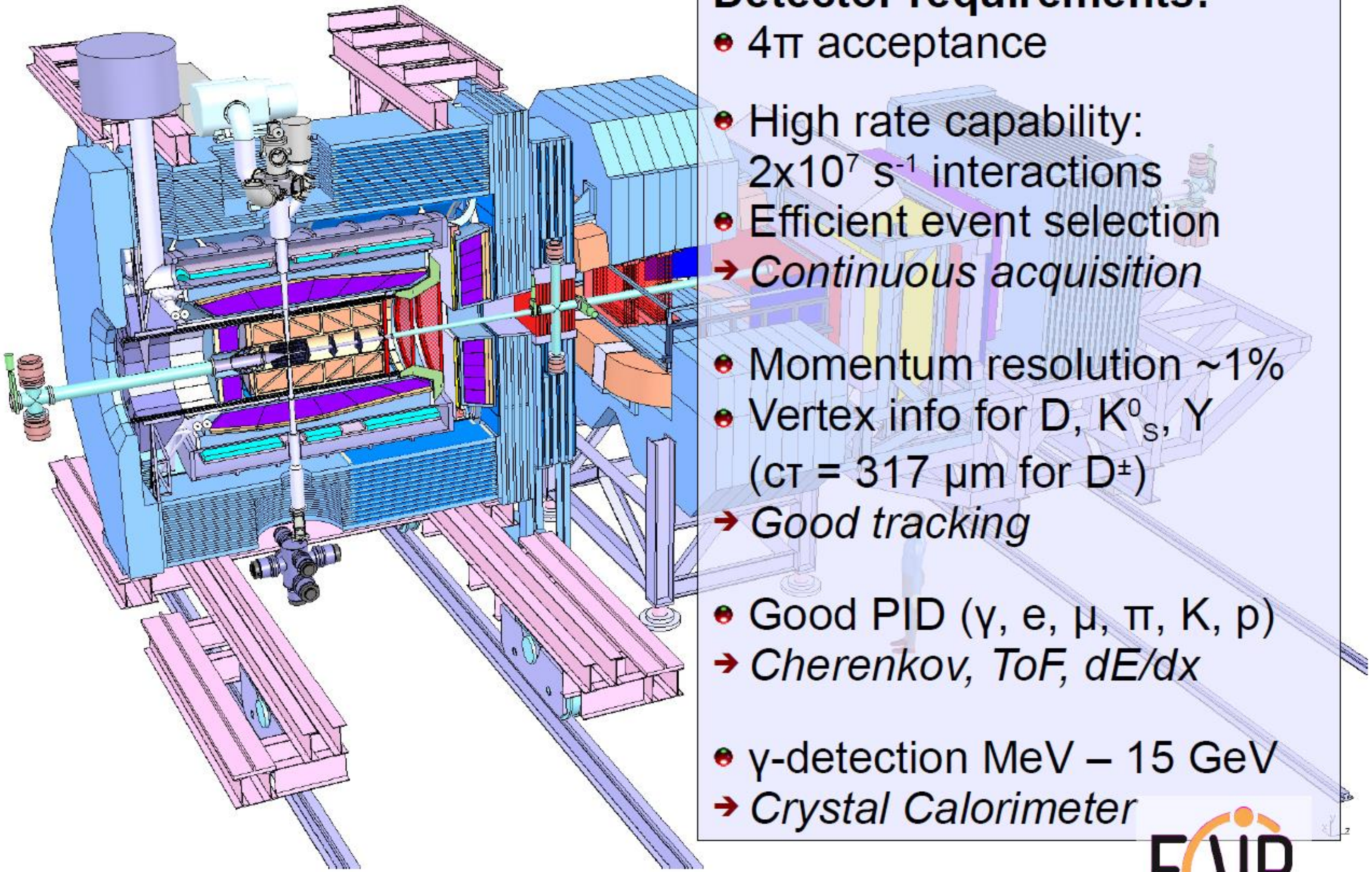

**Detector requirements:**

- 4π acceptance
- High rate capability: $2\times10^{7}\ s^{-1}$ interactions
- Efficient event selection

➔ *Continuous acquisition*

- Momentum resolution ~1%
- Vertex info for D, $K^0_S$, Y ($c\tau$ = 317 μm for $D^{\pm}$)

➔ *Good tracking*

- Good PID (γ, e, μ, π, K, p)

➔ *Cherenkov, ToF, dE/dx*

- γ-detection MeV – 15 GeV

➔ *Crystal Calorimeter*

# NICA at JINR

# basic facility

# major milestones

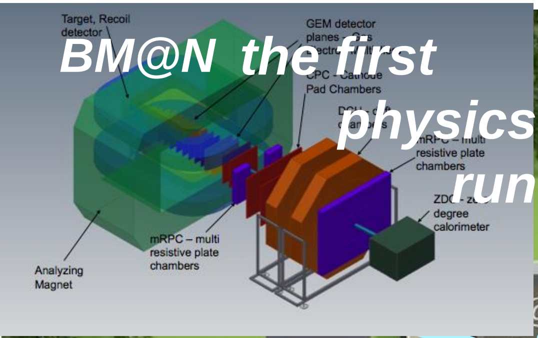


***BM@N the first physics run***

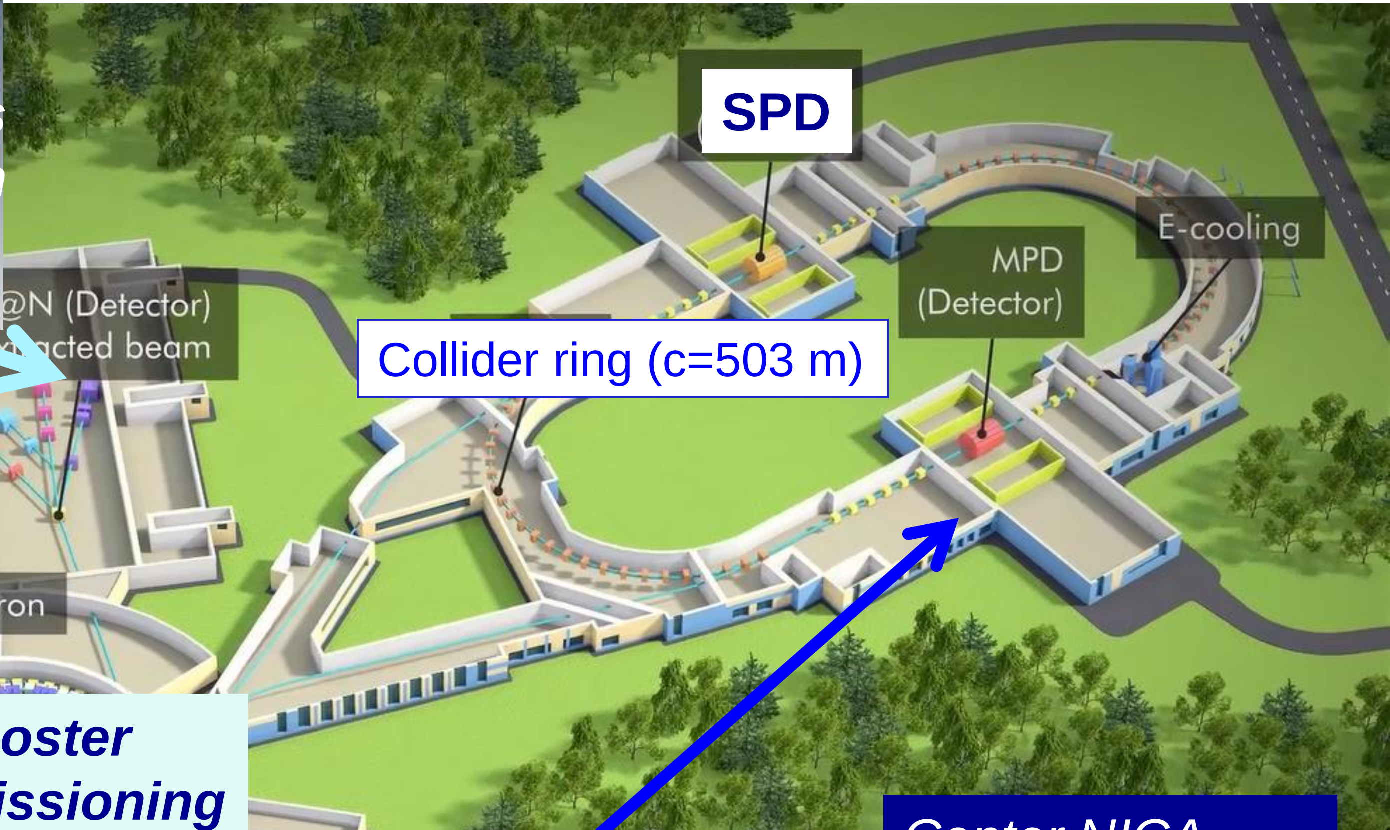


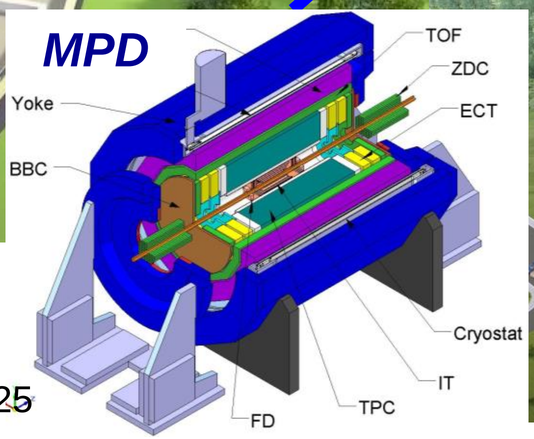


# SPD Hybrid system

½ model symmetry

$B^{(z)}(x,y,0)=0.$

$J_T = 40\frac{A}{mm^2},$

$J^{(1,2)}_{B\backslash F} = \mp 80\frac{A}{mm^2},$

$S = 200\times 20\,mm^2,$

$I_T = J_T \cdot S = 160\,kA,$

$I_{B\backslash F} = J_{B\backslash F}\cdot S = \mp 320\,kA.$

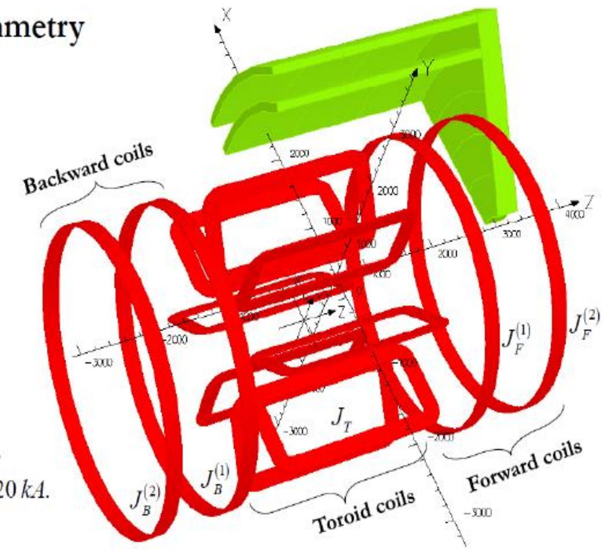


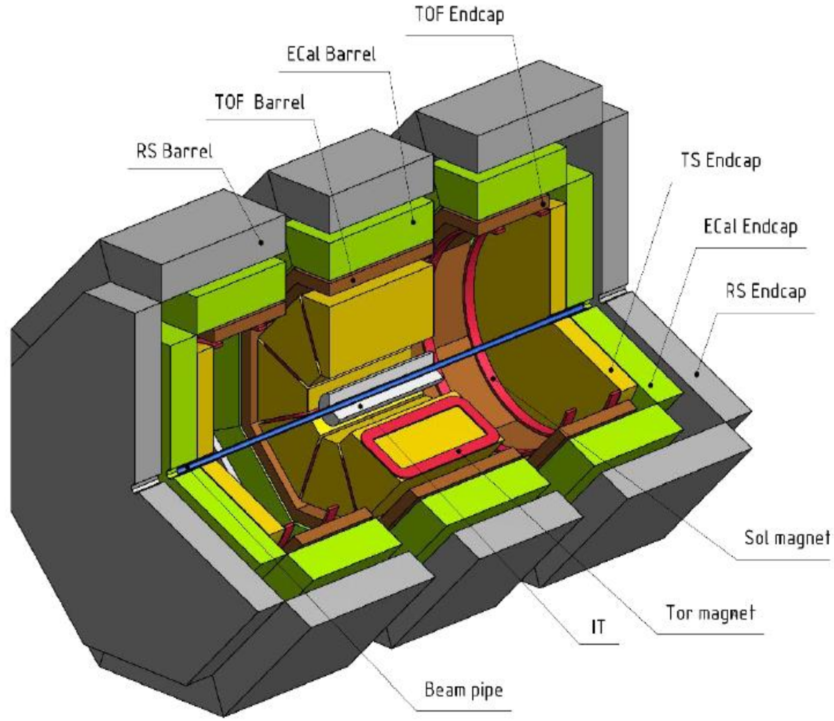


$$\Omega=\left\{(r,\varphi,z):\begin{array}{c}0\le r\le 3000\\ \varphi=0\\ 0\le z\le 3400\end{array}\right\}$$

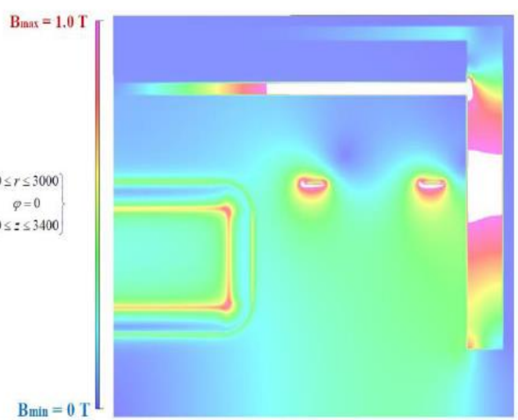


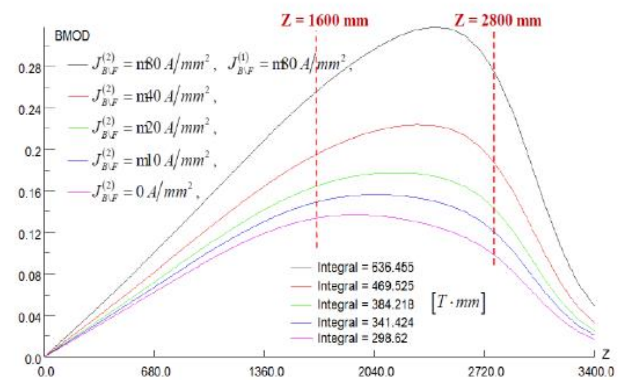

# Main advantages

**Unique beams: – wide range of kind of the beam particles (antiproton and polarization) and $\Delta p/p$ up to $10^{-5}$.**

**Unique detectors: $\Delta\Omega \sim 4\pi$ (exclusive reactions, correlations); detection of all kinds of particles; working at luminosity ~ $10^{32}$ $cm^{-2}$ $s^{-1}$ (rare events can be investigated); PID – close to full energy range and high momentum resolution.**

From the inclusive experiments to the correlations and the exclusive experiments

# DIQUARK NUCLEON COMPONENT

# Way to resolve these problems MPI and Exclusive reaction

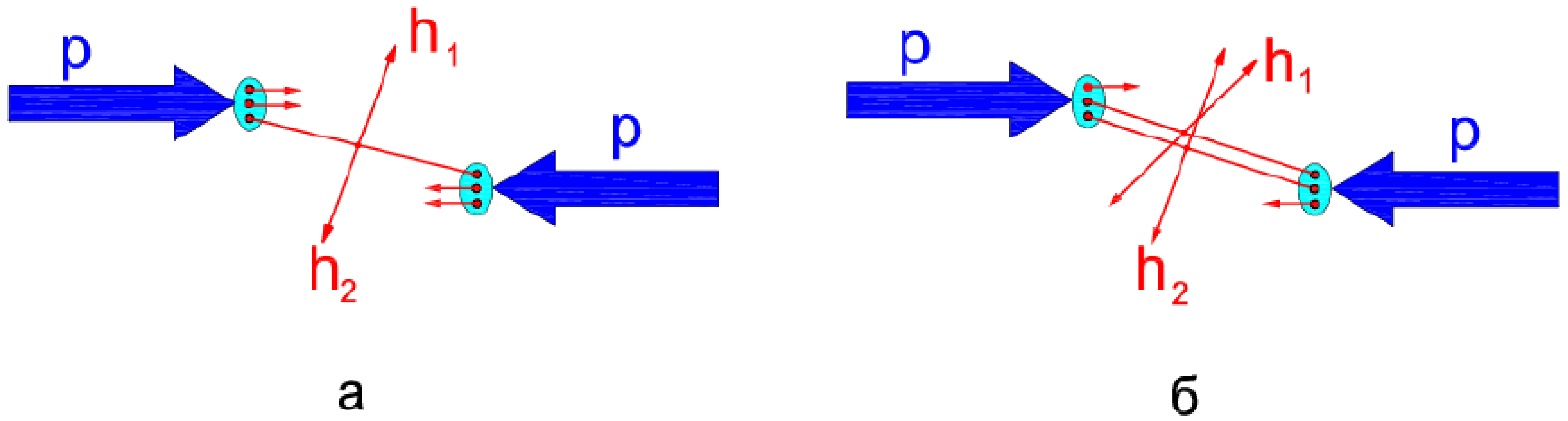

# Exclusive NN study at $x_T \sim 1$

$$N\uparrow + N\uparrow \rightarrow BB + MM$$

$B\,(p, n, \Lambda, \Delta \ldots)$, $M\,(\pi, K, \ldots)$

Mechanisms of hyperons polarization

$$N\uparrow N\uparrow \rightarrow NN$$

The counting rules and isotopic symmetry studies, $p_T \sim 2$ GeV/c anomaly

$$N\uparrow N\uparrow \rightarrow BB + \pi\pi(KK)$$

$$N\uparrow N\uparrow \rightarrow \Delta\Delta$$

Detail vertexes studies and spin structure of the interaction vertex:

$q + (q) - (quark - quark)$

$q + (qq) - (quark - diquark)$

$(qq) + (qq) - (diquark - diquark)$

# Kim's mechanisms in exclusive reactions

## pp - > pp + X, pp -> D(H, NΛ...) + X reactions with diquarks

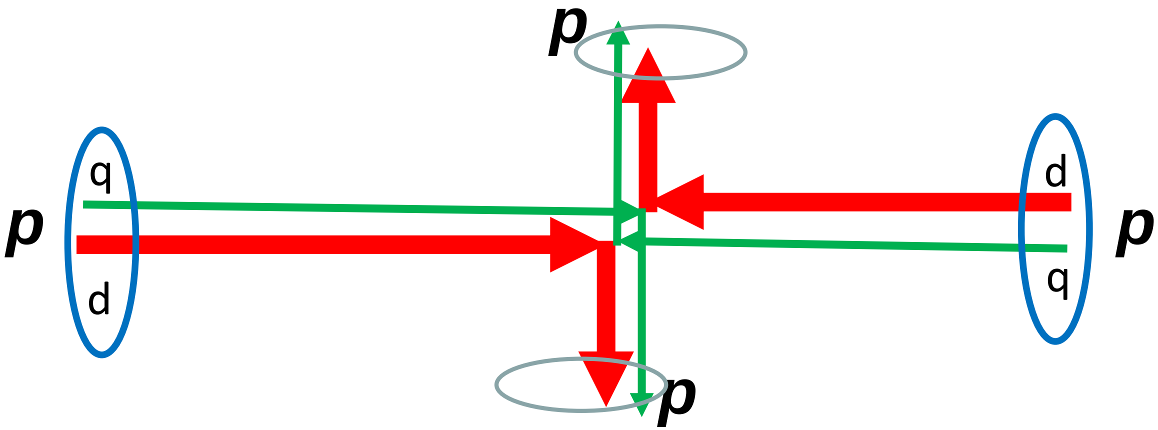


Double *qd*-scatering

Diquark proof

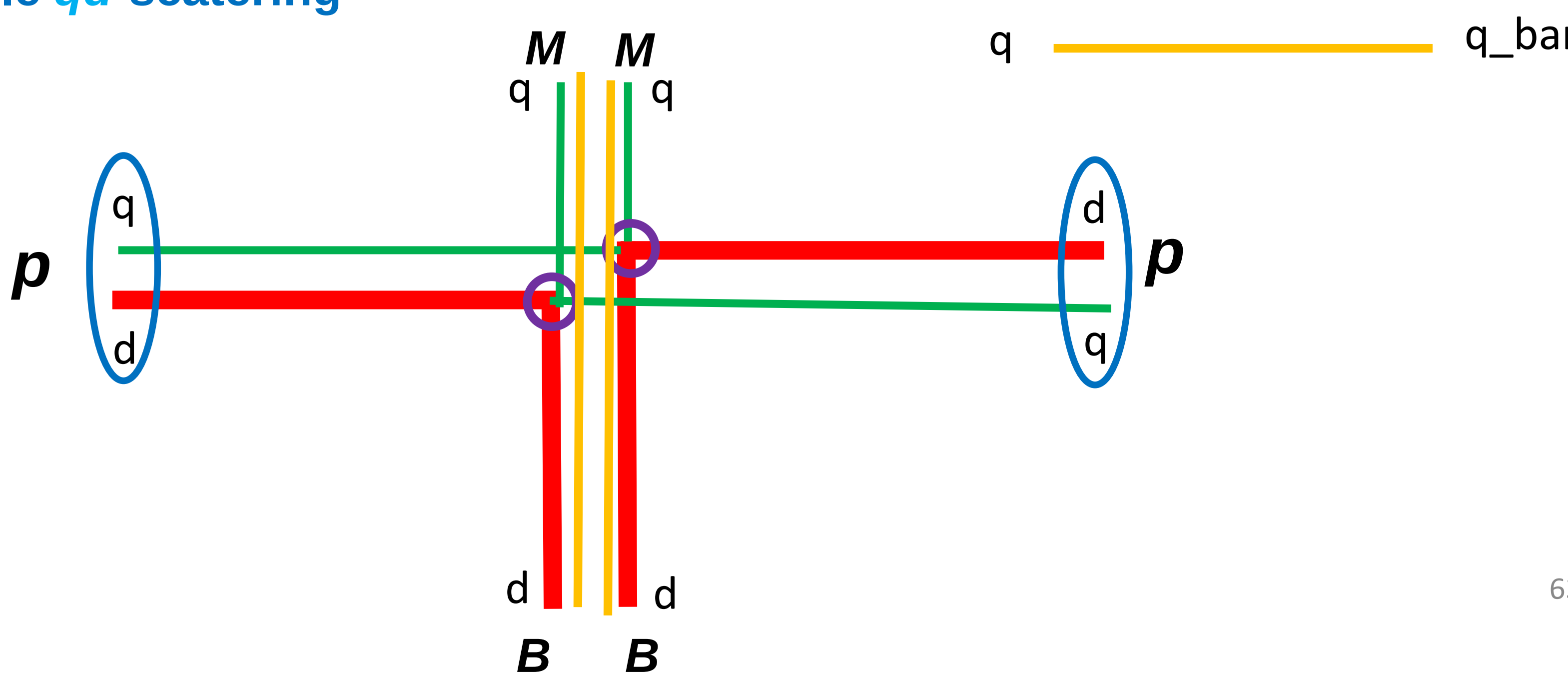

# High $p_T$ exclusive reactions -> MPI

$$p\uparrow + p\uparrow \to B + B + M\overline{M}$$

$$p\uparrow + p\uparrow \to p + p + \pi^0\pi^0(\pi^+\pi^-)$$

$$R = \frac{N(\pi^+\pi^-)}{N(\pi^0\pi^0)} = \frac{2}{7}$$ Without diquark

$$R = \frac{N(\pi^+\pi^-)}{N(\pi^0\pi^0)} \to 0$$ diquark

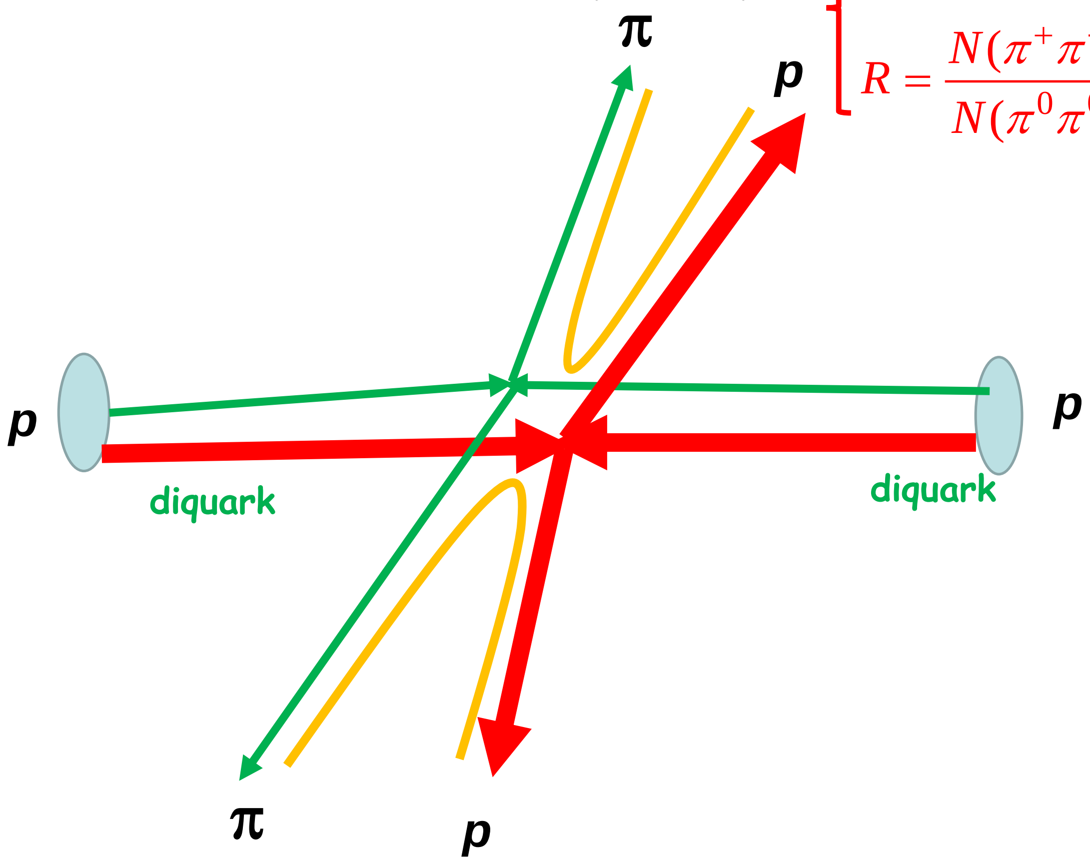


Diquark (S=0)

$$A_{n(pp)} \to 0$$

# Exotic states and flavor universality

# Kim's-bar mechanisms

# $\bar{p}p$ - reactions with tetraquarks production in

d – diquark !

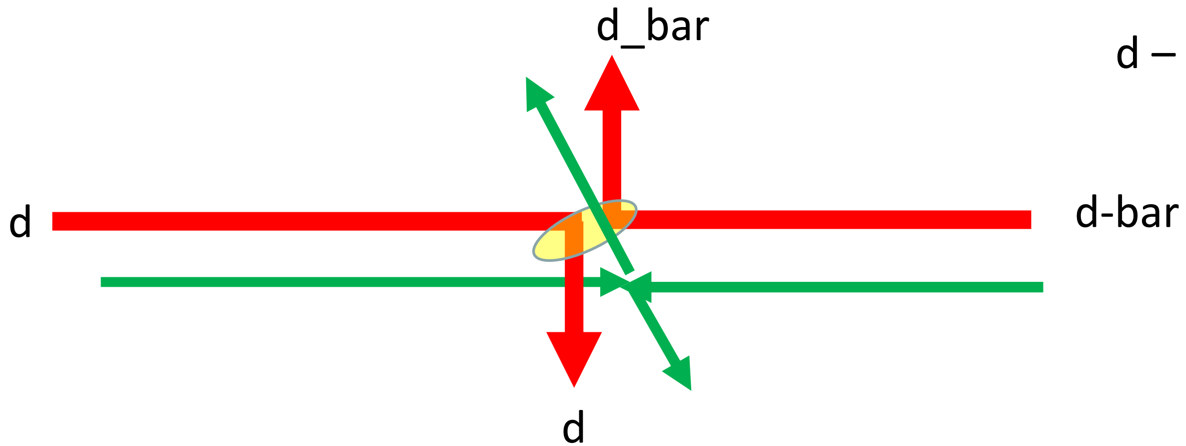


Diquark proof

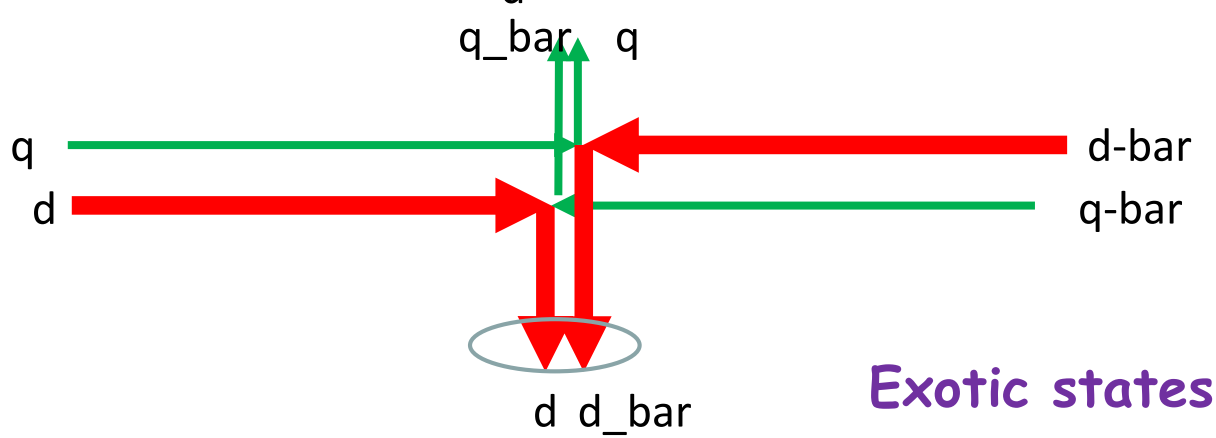


Exotic states production

# $\overline{p}d$ - reaction with tetraquarks +pentaquark production

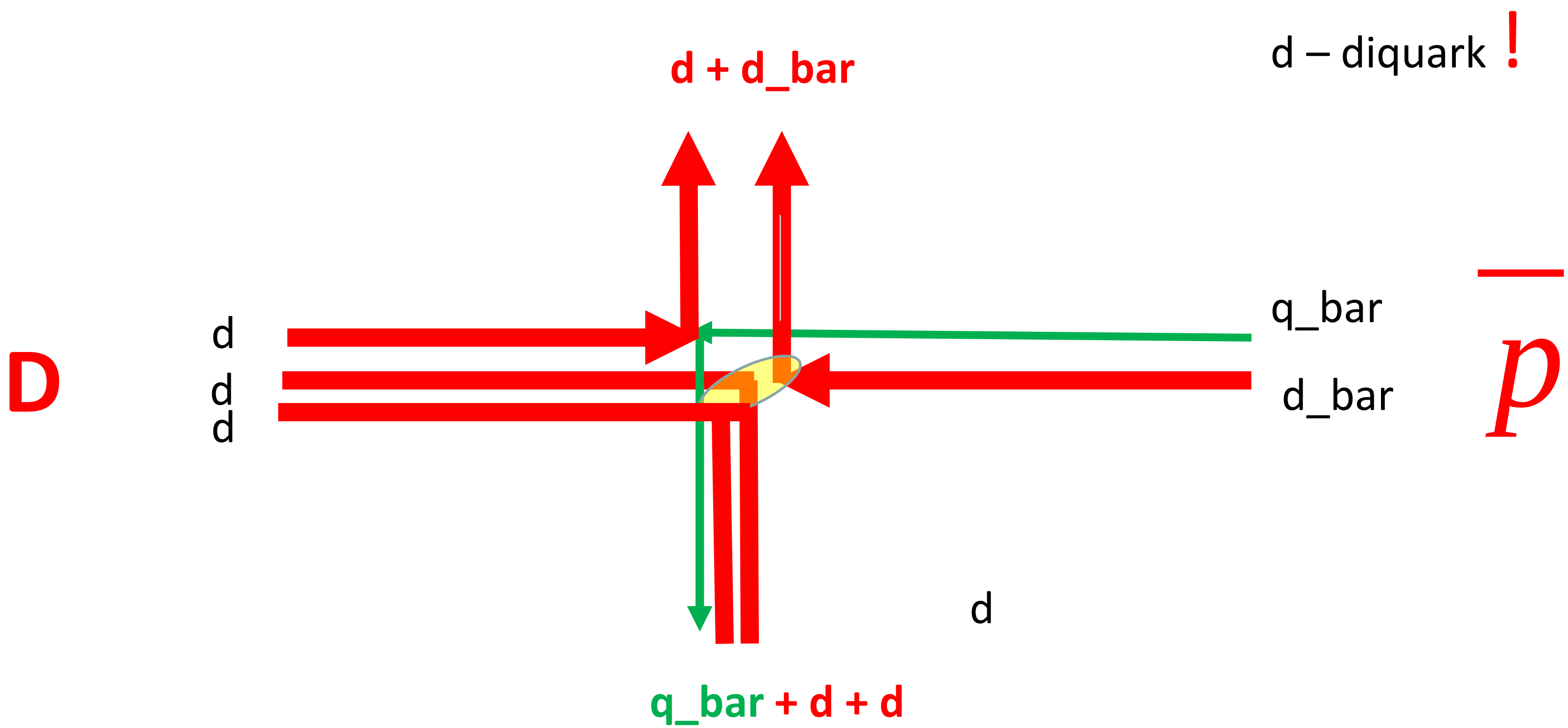

# Exotic states production

## pp - reactions with pentaquarks production

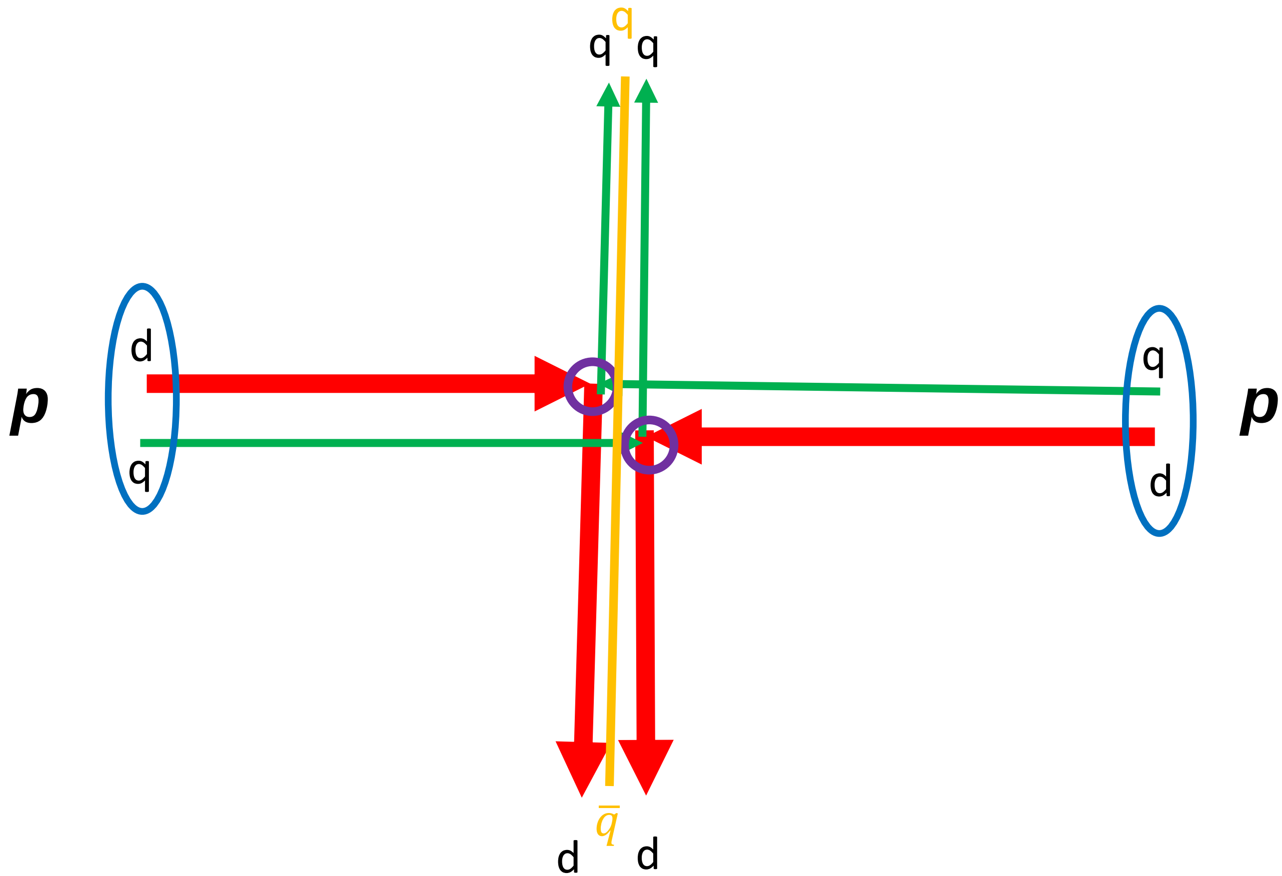

# Exotic states production

## pp - reactions with tetraquarks production

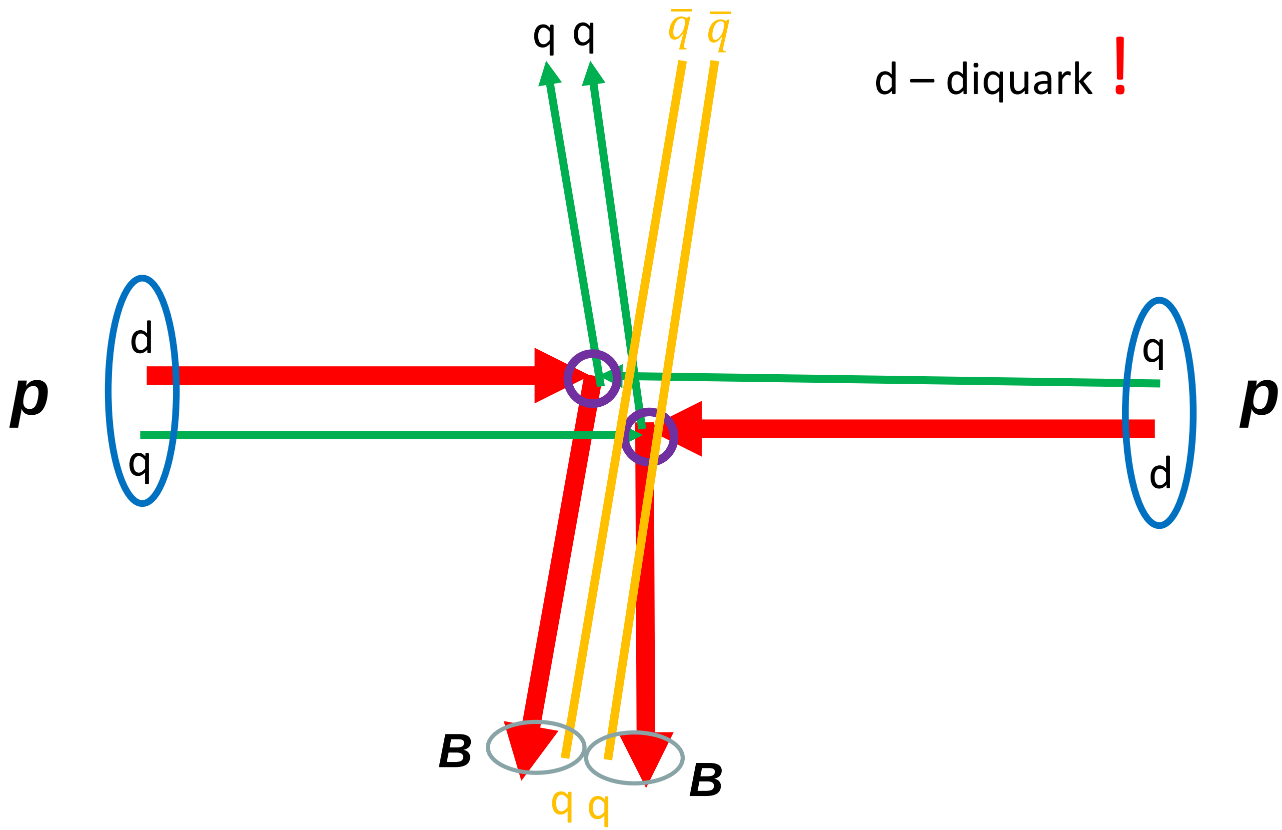

TABLE I. Proton-proton elastic scattering cross sections at 90° in the center-of-mass system.

| $P_{c.m.}^2$ $(GeV/c)^2$ | $P_0$ $(GeV/c)$ | $(d\sigma/d\Omega)_{c.m.}$ $(\mu b/sr)$ | $(d\sigma/dt)_{c.m.}$ $\mu b/(GeV/c)^2$ | Error in $d\sigma/d\Omega$ & $d\sigma/dt$ % |
|---|---|---|---|---|
| 1.946 | 5.0 | 8.51 | 13.74 | 2.9 |
| 1.993 | 5.1 | 7.90 | 12.45 | 3.3 |
| 2.039 | 5.2 | 7.09 | 10.93 | 3.1 |
| 2.086 | 5.3 | 6.49 | 9.77 | 3.6 |
| 2.132 | 5.4 | 5.53 | 8.15 | 3.1 |
| 2.178 | 5.5 | 4.90 | 7.07 | 3.4 |
| 2.223 | 5.6 | 4.47 | 6.32 | 3.1 |
| 2.270 | 5.7 | 3.72 | 5.15 | 3.3 |
| 2.316 | 5.8 | 3.37 | 4.57 | 3.3 |
| 2.363 | 5.9 | 2.74 | 3.64 | 3.5 |
| 2.409 | 6.0 | 2.44 | 3.18 | 3.1 |
| 2.456 | 6.1 | 2.19 | 2.80 | 3.7 |
| 2.503 | 6.2 | 1.83 | 2.30 | 3.7 |
| 2.595 | 6.4 | 1.50 | 1.82 | 3.7 |
| 2.686 | 6.6 | 1.07 | 1.25 | 4.7 |
| 2.779 | 6.8 | 0.796 | 0.900 | 4.7 |
| 2.873 | 7.0 | 0.645 | 0.706 | 4.1 |
| 2.965 | 7.2 | 0.515 | 0.546 | 4.0 |
| 3.059 | 7.4 | 0.386 | 0.396 | 4.8 |
| 3.151 | 7.6 | 0.305 | 0.304 | 5.4 |
| 3.247 | 7.8 | 0.253 | 0.245 | 4.5 |
| 3.338 | 8.0 | 0.217 | 0.204 | 4.5 |
| 3.386 | 8.1 | 0.169 | 0.157 | 3.9 |
| 3.434 | 8.2 | 0.172 | 0.157 | 4.4 |
| 3.480 | 8.3 | 0.154 | 0.139 | 3.8 |
| 3.527 | 8.4 | 0.153 | 0.136 | 4.6 |
| 3.618 | 8.6 | 0.127 | 0.110 | 4.6 |
| 3.713 | 8.8 | 0.103 | 0.0871 | 4.8 |
| 3.806 | 9.0 | 0.0809 | 0.0667 | 4.6 |
| 3.897 | 9.2 | 0.0780 | 0.0629 | 4.3 |
| 3.992 | 9.4 | 0.0676 | 0.0532 | 5.3 |
| 4.084 | 9.6 | 0.0589 | 0.0453 | 4.9 |
| 4.178 | 9.8 | 0.0536 | 0.0403 | 4.7 |
| 4.272 | 10.0 | 0.0468 | 0.0344 | 4.9 |
| 4.364 | 10.2 | 0.0441 | 0.0318 | 4.8 |
| 4.461 | 10.4 | 0.0386 | 0.0272 | 4.7 |
| 4.554 | 10.6 | 0.0356 | 0.0246 | 4.8 |
| 4.644 | 10.8 | 0.0303 | 0.0205 | 4.9 |
| 4.739 | 11.0 | 0.0284 | 0.0188 | 5.5 |
| 4.831 | 11.2 | 0.0255 | 0.0166 | 5.4 |
| 4.924 | 11.4 | 0.0202 | 0.0129 | 5.4 |
| 5.018 | 11.6 | 0.0190 | 0.0119 | 5.2 |
| 5.112 | 11.8 | 0.0153 | 0.00940 | 5.4 |
| 5.208 | 12.0 | 0.0143 | 0.00862 | 5.4 |
| 5.299 | 12.2 | 0.0118 | 0.00699 | 5.3 |
| 5.392 | 12.4 | 0.0116 | 0.00676 | 5.4 |
| 5.490 | 12.6 | 0.00953 | 0.00545 | 6.3 |
| 5.579 | 12.8 | 0.00867 | 0.00488 | 5.7 |
| 5.674 | 13.0 | 0.00739 | 0.00409 | 5.9 |
| 5.770 | 13.2 | 0.00722 | 0.00393 | 7.1 |
| 5.861 | 13.4 | 0.00525 | 0.00281 | 5.7 |

**The rate for $L \sim 10^{30}\ cm^{-2}c^{-1}$:**

$\sim 0.2\ c^{-1}$

$\sim 0.01\ c^{-1}$

# NICA Collision place for SPIN physics (deuteron and other beams, the first time all isotope states for NN system: pp, pn,nn.)

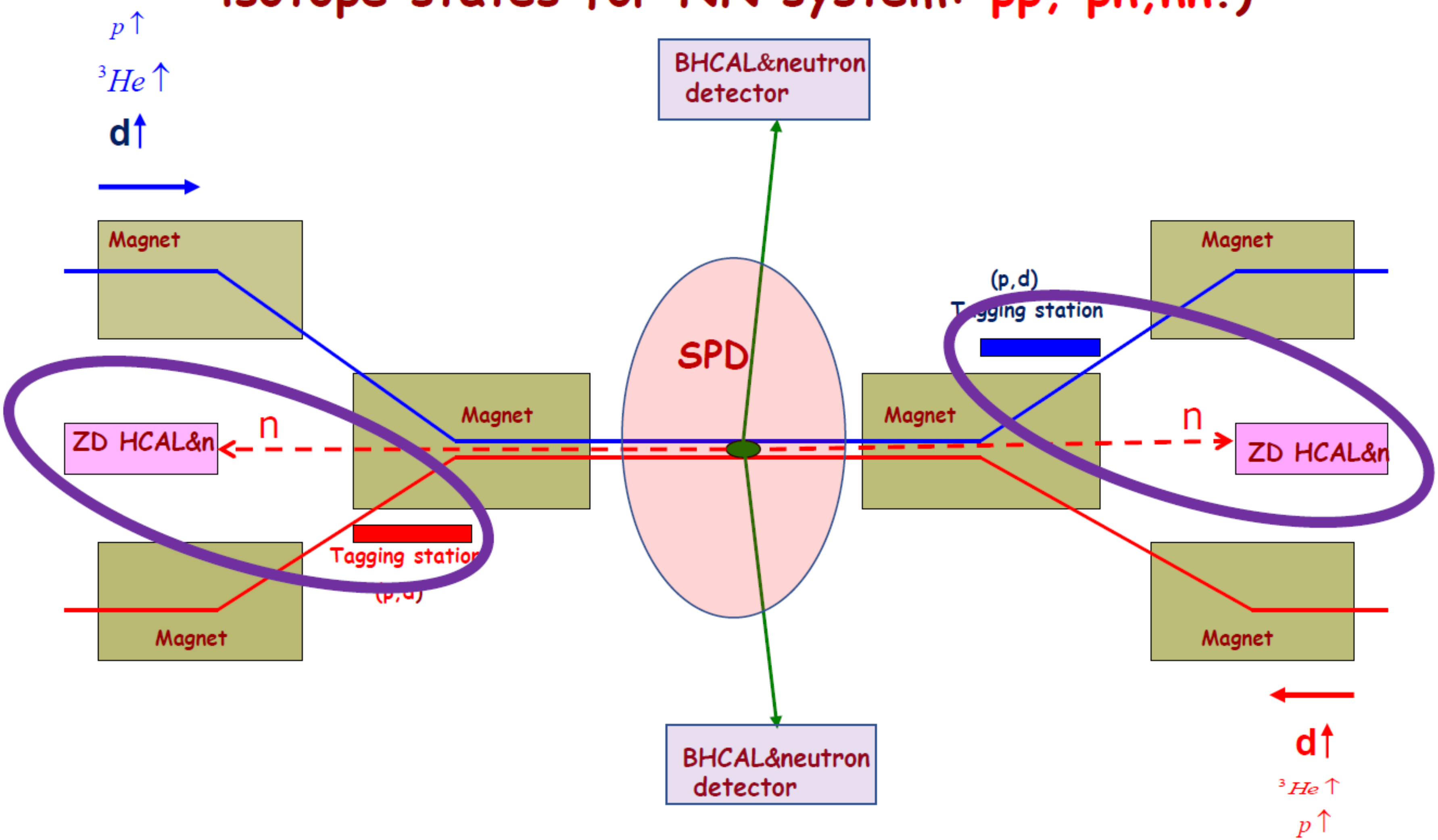


The tagging stations can be used as polarimeter!

END

| | |
|---|---|
| Тема | Re: Cumulative at high p_T |
| От | Boris Kopeliovich |
| Кому | Stepan |
| Ответить | bzk@mpi-hd.mpg.de |
| Дата | 23.01.2012 7:42 |

«I think that the main problem in understanding of high p_T hadrons at the energies of Serpukhov is why you see more protons than pions. This was claimed long time ago by the Sulyaev's group and I remember hot debates in that back in the 80s. Those debated ended up with no clear conclusion. Much later an excess of baryons was observed by the STAR at RHIC and was called "baryon anomaly". Again, no good explanation has been proposed so far. I might have my own explanation, but haven't written anything so far. Anyway, my point is, if we do not understand the mechanism of production of baryons dominating at high p_T, we should not make any certain conclusions about the cumulative mechanisms».